

## REPORT DOCUMENTATION PAGE

AFRL-SR-BL-TR-99-

Public reporting burden for this collection of information is estimated to average 1 hour per response, including the time for reviewing instructions, the collection of information. Send comments regarding this burden estimate or any other aspect of this collection of information, including Operations and Reports, 1215 Jefferson Davis Highway, Suite 1204, Arlington, VA 22202-4302, and to the Office of Management and Budget, P

and reviewing  
information

1. AGENCY USE ONLY (Leave blank)		2. REPORT DATE	3. REPORT TYPE AND DATES COVERED 01 Mar 98 to 31 Jul 99 Final	
4. TITLE AND SUBTITLE DURIP-98-99 Test facility for Atmospheric Pressure Plasmas			5. FUNDING NUMBERS 61103D 3484/US	
6. AUTHOR(S) Dr Schoenbach				
7. PERFORMING ORGANIZATION NAME(S) AND ADDRESS(ES) Old Dominion University Research Foundation 800 West 46th Street P O Box 6369 Norfolk, VA 23508-0369			8. PERFORMING ORGANIZATION REPORT NUMBER	
9. SPONSORING/MONITORING AGENCY NAME(S) AND ADDRESS(ES) AFOSR/NE 801 North Randolph Street Rm 732 Arlington, VA 22203-1977			10. SPONSORING/MONITORING AGENCY REPORT NUMBER  F49620-98-1-0347	
11. SUPPLEMENTARY NOTES			19991119 085	
12a. DISTRIBUTION AVAILABILITY STATEMENT APPROVAL FOR PUBLIC RELEASED; DISTRIBUTION UNLIMITED			12b. DISTRIBUTION CODE	
13. ABSTRACT (Maximum 200 words)  In order to compare the various proposed methods of plasma generation in high pressure gases, particularly air, a test facility for atmospheric pressure plasmas has been established. The facility is located in the Applied Research Center of Old Dominion University (ODU), in Newport News, VA. The diagnostic instrumentation at the facility allows us to determine the electrical parameters of high pressure glow discharges, the temporal development of instabilities, the electron density, and the temperature at high spatial (micrometer) and temporal (ns) resolution. Diagnostic techniques developed under this grant are gas temperature measurements in air, based on the emission spectroscopy (rotational spectrum of the second positive system of nitrogen) and electron density measurements using a CO <sub>2</sub> interferometer. In addition a 105 GHz microwave interferometer has been acquired and is available for measurements where a spatial resolution of only mm is required.				
14. SUBJECT TERMS			15. NUMBER OF PAGES	
			16. PRICE CODE	
17. SECURITY CLASSIFICATION OF REPORT  UNCLASSIFIED	18. SECURITY CLASSIFICATION OF THIS PAGE  UNCLASSIFIED	19. SECURITY CLASSIFICATION OF ABSTRACT  UNCLASSIFIED	20. LIMITATION OF ABSTRACT  UL	

DTIC QUALITY INSPECTED 4

Standard Form 298 (Rev. 2-89) (EG)  
Prescribed by ANSI Std. Z39.18  
Designed using Perform Pro, WHS/DIOR, Oct 94

**Final Report**  
**on the Project**  
**TEST FACILITY FOR ATMOSPHERIC**  
**PRESSURE PLASMAS**

**Grant No: F49620-98-1-0347**

submitted to

**Dr. Robert J. Barker**

**Air Force Office of Scientific Research**  
**801 N. Randolph St.**  
**Arlington, VA 22203-1977**  
**Tel.: (703) 696-8574**  
**FAX: (703) 696-8481**  
**E-mail: robert.barker@afosr.af.mil**

by

**Karl H. Schoenbach**

**Physical Electronics Research Institute**  
**Old Dominion University**  
**Norfolk, VA 23529**  
**Tel.: (757) 683-4625**  
**FAX: (757) 683-3220**  
**E-mail: schoenbach@ece.odu.edu**

## ABSTRACT

The importance of partially ionized gases at atmospheric pressure for defense and for commercial applications has lead to strong research activities at several universities and industry laboratories. In order to compare the various proposed methods of plasma generation in high pressure gases, particularly air, a test facility for atmospheric pressure plasmas has been established. The facility is located in the Applied Research Center of Old Dominion University (ODU), in Newport News, VA. The diagnostic instrumentation at the facility allows us to determine the electrical parameters of high pressure glow discharges, the temporal development of instabilities, the electron density, and the gas temperature at high spatial (micrometer) and temporal (ns) resolution. Diagnostic techniques developed under this grant are gas temperature measurements in air, based on the emission spectroscopy (rotational spectrum of the second positive system of nitrogen) and electron density measurements using a CO<sub>2</sub> interferometer. In addition a 105 GHz microwave interferometer has been acquired and is available for measurements where a spatial resolution of only mm is required. The facility will provide researchers in the AFOSR funded Air Plasma Rampart Program, the major research initiative in the nonthermal high-pressure plasmas, the opportunity to compare plasma generation methods with respect to efficiency and stability in a standardized discharge cell.

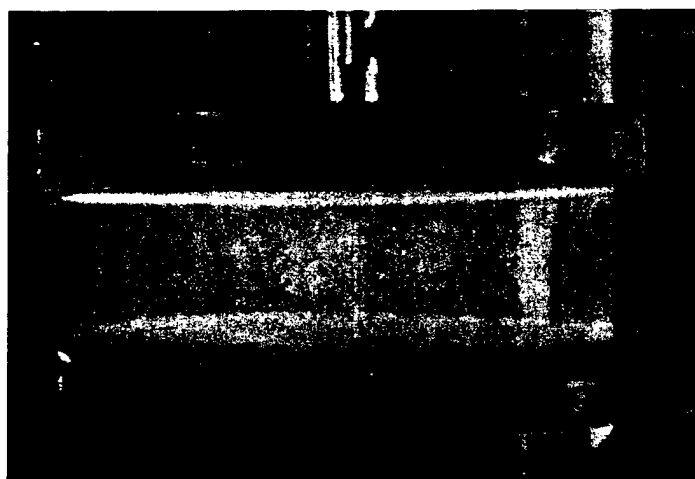
## High Pressure Plasmas

Plasma "Ramparts", weakly ionized plasmas, which serve as shields against electromagnetic radiation, are the topic of a Multi-University Research Initiative (MURI) directed by AFOSR with Dr. R. Barker as Program Manager. The goal of the Air Plasma Ramparts Program which includes scientists of more than fifteen research institutions is to obtain a fundamental physical understanding for the efficient generation and maintenance of a plasma with an electron concentration of  $10^{13} \text{ cm}^{-3}$  in air at atmospheric pressure. Besides their importance for plasma ramparts, atmospheric pressure plasmas have a variety of industrial applications. These are pollutant remediation, material deposition, surface cleaning, curing of polymers and others.

The two basic methods which can be used to generate large volumes of weakly ionized gas in high pressure gases are:

1. external ionization (by means of photons or charged particles, generally electron-beams), and
2. internal ionization, the generation of electrons and ions in a self-sustained discharge. Examples of this kind are RF and microwave, discharges, barrier discharges, and pulsed corona discharges, where the discharge is sustained by pulsed and alternating fields, and steady-state discharges, where the discharge is driven by a dc power source. The need for high efficiency might require for either method the injection of seed gases suitable for photo ionization, combustible gases or small particles.

At the Physical Electronics Research Institute at Old Dominion University (ODU) we have concentrated on two types of self-sustained high-pressure glow discharges. One is an ac driven discharge [1] with estimated electron densities of  $10^9$  to  $10^{10} \text{ cm}^{-3}$ . A typical plasma generated with such a method is shown in figure 1. The second type of high pressure plasmas, studied at ODU, is the microhollow cathode sustained glow [MCSG] [2] which has electron densities close to  $10^{13} \text{ cm}^{-3}$ , but has a much smaller volume than the ac discharge. An example for such a discharge is shown in Fig. 2. Large volume plasmas, however, can be generated by superposition of individual MCSGs. Tests of the various diagnostic techniques available at the test facility have been performed on these two types of atmospheric pressure plasmas.



Gas: air + helium  
 Dimensions: Gap = 3 cm  
 Frequency: 20 kHz  
 Voltage: 5kV (RMS)  
 Current : 50 mA

**Fig. 1 Atmospheric Pressure Glow Discharge**

**Estimated Plasma Parameters:**

Electron density:  $10^9 \text{ cm}^{-3} - 10^{10} \text{ cm}^{-3}$   
 Gas Temperature:  $< 500 \text{ K}$

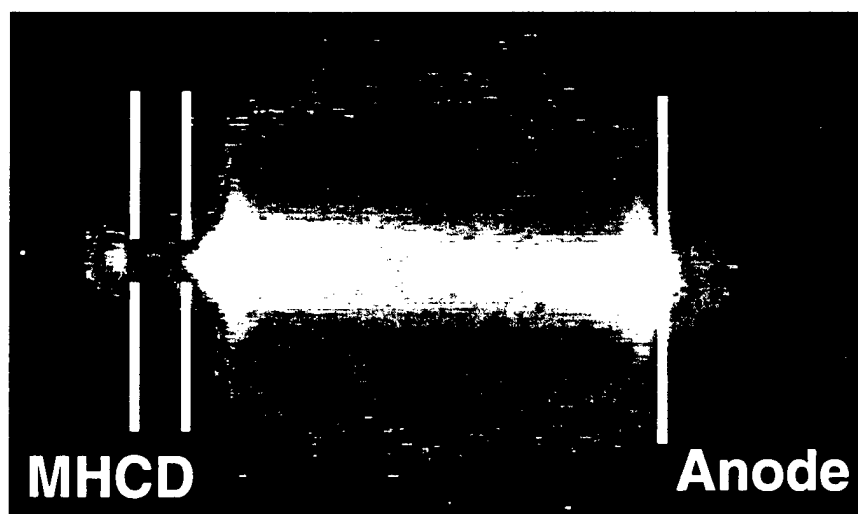


**Fig. 2 Atmospheric Pressure, MCS Glow Discharge**

<b>Mode of Operation:</b>	Direct Current	<b>Current Density:</b>	$J = 3.8 \text{ A/cm}^2$
<b>Dimensions:</b>	Gap = 2 mm	<b>Electric Field:</b>	$E = 1.2 \text{ kV/cm}$
<b>Voltage:</b>	$V = 238 \text{ V}$	<b>Drift velocity:</b>	$v = 5 \cdot 10^6 \text{ cm/s}$
<b>Current:</b>	$I = 22 \text{ mA}$		
<b>Temperature:</b>	$T \cong 2,000 \text{ K}$		$\rightarrow \text{Electron Density: } 5 \cdot 10^{12} \text{ cm}^{-3}$

## **Diagnostic Techniques for High Pressure Plasmas, Developed or under Development at the Test Facility**

A set of diagnostic techniques, appropriate for the evaluation of APRP plasmas has been discussed and documented. Contributors to the "Recipe Booklet" were, besides the P.I. of this project, Charles Krueger and Christophe Laux of Stanford, Erich Kunhardt of Stevens Institute of Technology, Richard Miles of Princeton, and Rolf Block and Olaf Toedter of Old Dominion University. The contributions have been edited, together with the P.I of this project, by Dan Kelley (Boeing). The topics of the booklet are a) electron density measurement techniques, and b) gas temperature measurement techniques. A list of the methods is depicted in Fig. 3. The one in red are those which have been developed, or under development in our test facility. An overview on the test facility and the diagnostic methods available at this facility was the topic of an invited talk [3] and a contributed conference presentation [4]. The abstract for the invited talk, which was presented at the 1999 ICOPS, and the paper [4] are enclosed.

### **1. Electrical Measurements (Electron Density)**

A method to obtain the electron density by measuring current density and electric field, and by using information on the electron drift velocity depending on the reduced electric field, has been discussed in the enclosed paper by Karl H. Schoenbach [5]. The method has been used to determine the electron density in microhollow cathode sustained glow discharges in atmospheric pressure air [6].

### **2. Microwave Interferometry (Electron Density)**

A 105 GHz microwave interferometer has been purchased, and is presently tested. A description of the system can be found in the section "Test Facility Equipment" in this report.

### **3. Emission Spectroscopy (rotational spectrum of the second positive system of nitrogen) (Gas Temperature)**

A diagnostic technique for the determination of the gas temperature was developed. It is based on emission spectroscopy (rotational spectrum of the second positive system of nitrogen). An introduction into this method was presented in an enclosed paper by O.Toedter and R. Block [7]. Olaf Toedter, a scientist from the University of the Saarland in Saarbruecken, Germany, has spent three months in 1987 in our labs, and has introduced this method to our research team. Rolf Block, a visiting professor from the Telekom Fachhochschule in Leipzig, Germany, was instrumental in implementing the

Recommendations for the measurement of the relevant parameters for APRP plasmas have been developed and have been (in part) documented in a "Recipe Booklet"

### **Electron Density**

- Electric Measurements
- Emission Spectroscopy (NO C state)
  
- Emission Spectroscopy ( $H\beta$  Stark broadening)
- Microwave Interferometry
- Thomson Scattering

### **Gas Temperature**

- Emission Spectroscopy (rotational states)
- Laser Absorption Spectroscopy
- Rayleigh Scattering

### **Electron Density and Gas Temperature**

- $CO_2$  Laser Interferometry

Fig. 3 Diagnostic Methods to determine Plasma Parameters in Atmospheric Pressure Air Plasmas

software for this method, and has performed the first measurements on high-pressure air plasmas using this technique. His paper on this topic is enclosed [8].

#### **4. Heterodyne Interferometry (Electron Density and Gas Temperature)**

This method is briefly described in the enclosed abstract [9]. The experimental set-up is shown in Fig. 4. A more detailed manuscript on this method is under preparation. Has been introduced to our research team by Frank Leipold, a visiting scientist on leave from the Institute for Low Temperature Plasma Physics (INP) in Greifswald, Germany. The equipment used for this diagnostics is on loan from the same institute.

#### **5. Other Diagnostic Techniques**

It is intended to add to this list of diagnostic methods, by exploring methods which were recommended and used by other members of the Plasma Rampart Consortium ("black" methods listed in Fig. 3). We plan particularly to develop a temperature diagnostics based on line broadening of argon as an additive to atmospheric pressure air [10]. An introduction to this method was written by O. Toedter. His manuscript is enclosed [11].

### **Research Facilities**

The test facility is located in the Applied Research Center on the campus of the Jefferson Laboratory in Newport News, VA. A view of the lab is shown in Fig. 5. A close-up which (Fig. 6) shows the vacuum chamber. The equipment used in this laboratory is described in the following section "Test Facility Equipment".

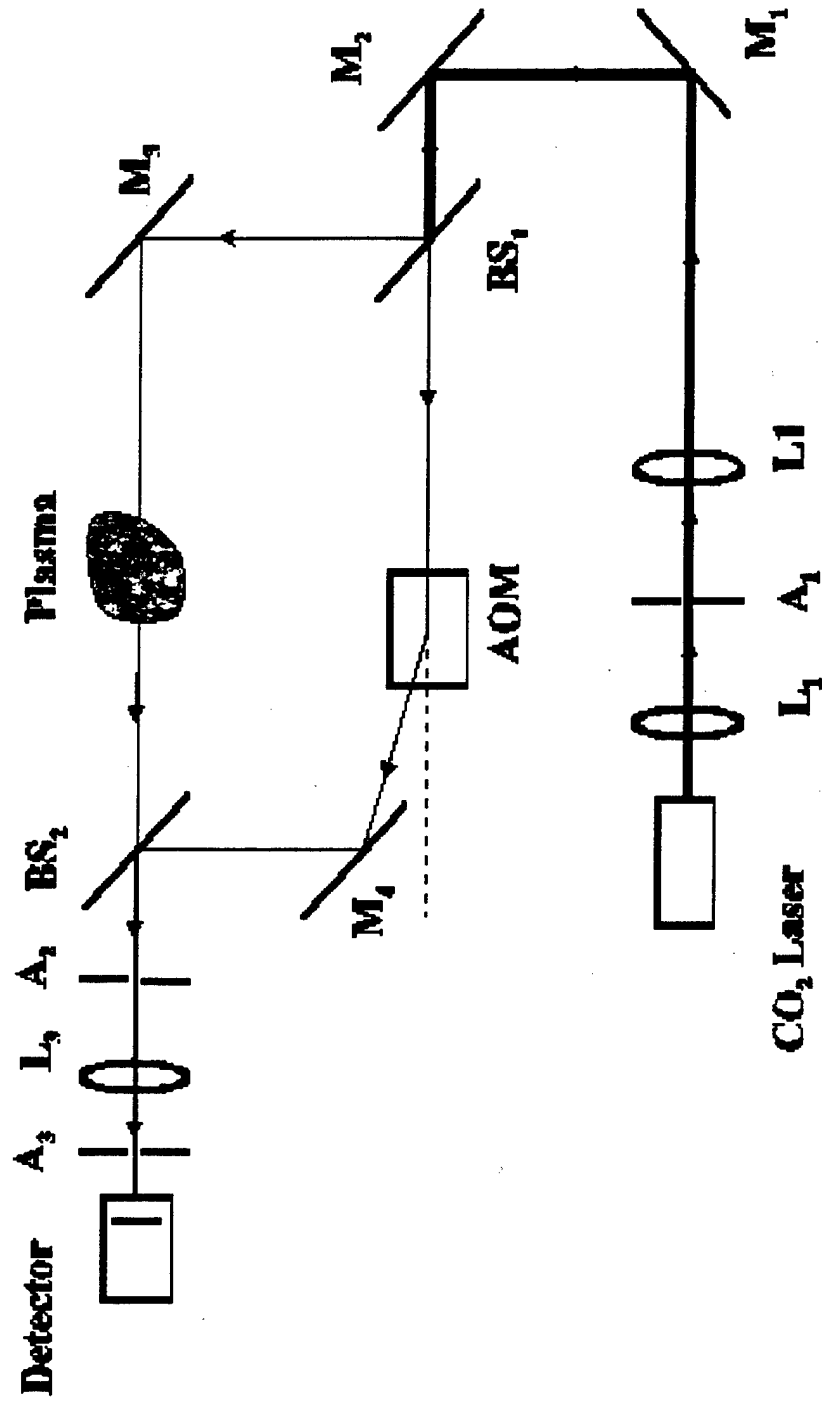
### **Test Facility Equipment**

#### **Discharge chamber, vacuum parts:**

The discharge chamber is a stainless steel vessel, 12" diameter, 11" high, with a total of 18 ports. All ports have CF-flanges. 4 CF 6 viewports (two with glass, two with quartz; view diameter: 3.97") can be used for optical diagnostics; a plasma with dimensions of 5 cm in all directions can be viewed in total through these viewports. Twelve CF 2.75 ports can be used for pressure sensors, gas feedthrough, liquid feedthrough (cooling water), electrical feedthrough (instrumentation and high voltage), smaller vacuum pumps or diagnostic equipment. Different types of feedthroughs, valves and other accessories are available. The CF 6 flange at the bottom is used for the main vacuum stand; a CF 6 valve can close this port. The CF 8 flange on top of the vessel is reduced to CF 2.75 to allow the feedthrough of a high voltage line.



Fig. 4 **Experimental Setup (Heterodyne Interferometry)**



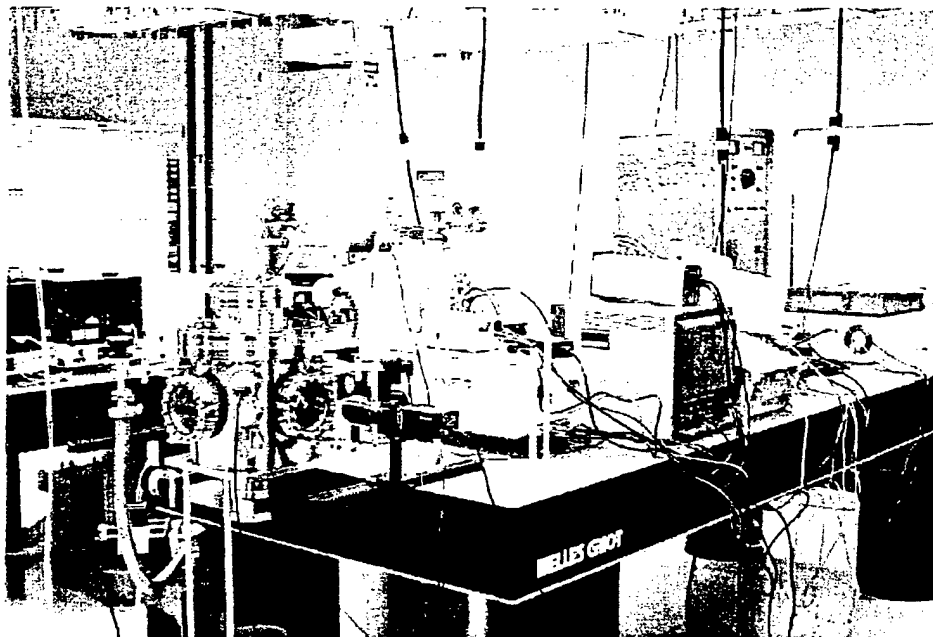


Fig. 5. View of Test Facility

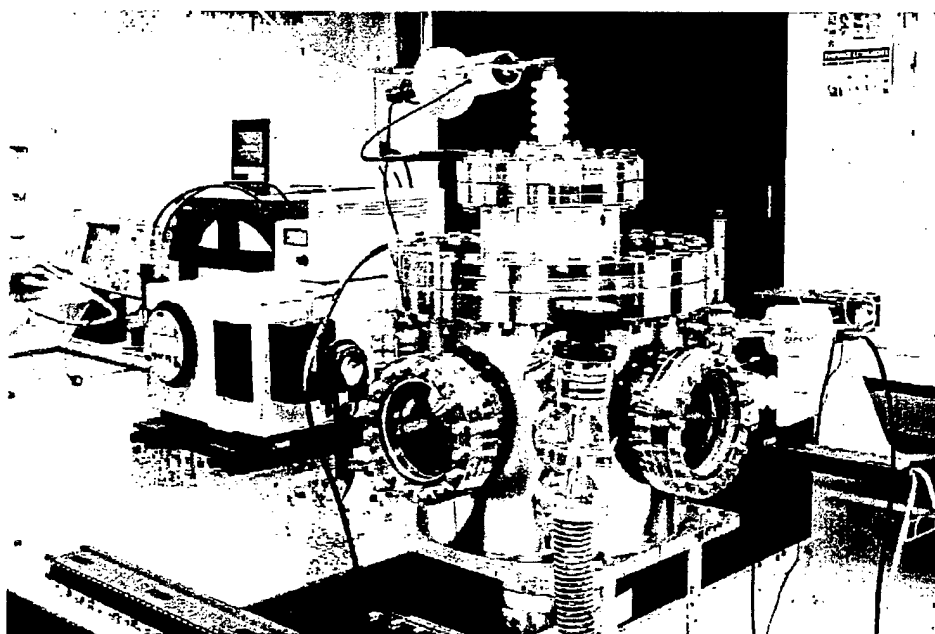


Fig. 6 Plasma Chamber

An oil-free dry pumping system consisting of a primary diaphragm pump and a secondary molecular drag pump for the pumping of corrosive gases with an ultimate pressure range of  $10^{-6}$  mbar is available. The primary pumping speed is 4 m<sup>3</sup>/h, the secondary pumping speed is about 20 l/s (dependant on gas). A second identical system can be used for differential pumping (residual gas analysis). Several diaphragm-operated vacuum-pressure pumps with single head and dual heads can be used for pressure, suction and gas circulating applications. A minimum pressure of about 50mbar is achievable with these pumps. A pressure gauge which combines three measurement methods – absolute pressure sensor, Pirani and Penning – covers the entire pressure range from  $10^{-9}$  to 2000 mbar. A Penningvac sensor covers the range from  $10^{-9}$  to  $10^{-2}$  mbar, a Thermovac sensor is used for pressures between  $5 \cdot 10^{-4}$  to 1000 mbar, and for most accurate measurements, independent of the type of gas, an absolute pressure sensor with a measurement range from  $5 \cdot 10^{-4}$  to 1,330 mbar is available. Regulators for different kinds of gases, needle valves, flow meters, coupling equipment and other accessories for gas handling allow adding of gases for combustion and other seed gas experiments.

### **Optical diagnostics:**

Spectra Pro 556, 0.5m Imaging Monochromator/Spectrograph with triple grating turret, 32-bit microprocessor controlled scanning. Scan range: 0 to 1400nm. Operating range: 185nm to the far infrared with available gratings and accessories. Resolution: 0.05nm at 435.8nm. Dispersion: 1.7nm/mm. Accuracy:  $\pm 0.2$ nm. Drive Step Size: 0.0025nm. One entrance slit and one exit slit, micrometer adjustable from 10 $\mu$ m to 3mm. One CCD output port with sliding tube CCD adapter. Two gratings are available: 1200g/mm grating with 500nm blaze wavelength, and 3600g/mm grating with 240nm blaze wavelength. Radiation is recorded by means of a Photomultiplier tube, 190-900nm range, and evaluated with a PC based data acquisition system. A variety of optical positioning equipment, mounts, holders and lenses are available.

Color CCD cameras (Panasonic, Sony; 768 horizontal pixels x 480 lines). Macro zoom video lens, 1mm to 108mm F/2.5. Microscope video lens, 1.4mm to 8.8mm FOV on 1/2" CCD, system magnification: 28X to 180X. 13" color monitors. SVHS Video Cassette Recorders. Video capture interface and software. Kodak digital still picture camera, 1536 x 1024 pixels resolution, auto focus zoom lens, 8mm to 24mm.

Light intensified CCD-camera for studying plasma ignition processes and the development of instabilities and for temporally resolved spectroscopic measurements (4 Picos).

Number of pixels: 768 x 494, EIA, 752 x 582 CCIR.

Resolution: 650 TV lines; 17 – 18 line pairs/mm.

25mm MCP with S20Q photocathode, 180nm – 820nm.

Sensitivity: 1 $\mu$ lux – 1nlux.

Shutter:  $t_s$  = 200ps ... 80s, min. steps 100ps

Delay:  $t_d$  = 0 ... 80s, min steps 100ps

Min. time between exposures: 0.33 $\mu$ s

Data acquisition system, PC, spectroscopy software.

### **Electrical diagnostics:**

Tektronix TDS640A, four channel digitizing oscilloscope, 400MHz, 2Gs/s.  
Tektronix TDS380, two channel digital real time oscilloscope, 400MHz, 2Gs/s.  
P6114B, 400MHz, 10x passive probes.  
P5100, 150MHz, 100x passive probes, 2500V.  
P6015A, 500kHz, 1000x high voltage probes, 20,000V.  
Various multimeters, partly with serial PC interface.

### **Power supplies (DC and pulsed):**

25kV, 400mA DC power supply. Output voltage is continuously adjustable. Continuously adjustable overload from 10 – 110 percent of rated current. Reversible polarity. Protection: solenoid driven, safety shorting switch.  
2 kV, 1A DC power supply. Output voltage and current are continuously adjustable from zero to the maximum rating. Reversible polarity. Remote monitor outputs for output voltage and current. Protection: overvoltage, overcurrent, arc and adjustable short circuit.  
Various low power, low voltage DC power supplies for electronic circuits, microwave phase bridge, etc.

10kV variable width pulse generator. Specifications are dependent on external load conditions. Voltage continuously adjustable from 500V to 10kV. Repetition rate continuously adjustable from  $10^{-1}$  to  $10^3$  hertz. Pulse width continuously adjustable from  $10^{-6}$  to  $10^{-2}$  seconds. Rise time (HiZ output) about 35ns (for 11k $\Omega$  load about 110ns). Fall time (HiZ output) about 18 $\mu$ s (for 11k $\Omega$  load about 2.4 $\mu$ s).

### **Microwave interferometer:**

I/Q phase bridge for electron density measurements. A Gunn oscillator provides 40mW of RF power at 105 GHz. A power divider provides 20mW to the transmit portion of the phase bridge, which contains a phase shifter and a level set attenuator. The remaining power is channeled to a second power divider which splits the signal to drive the two I-Q mixers providing coherency. The receiving portion gathers the RF signal transmitted through the plasma. The signal power is divided and provides the RF signals to the mixers. Because both mixer input signals are at the same frequency and from the same source, the output is DC. Electron densities up to about  $7 \cdot 10^{13} \text{ cm}^{-3}$  can be measured

### **Equipment available for the test facility, but not purchased with DURIP funds:**

1. Nd:YAG-laser (energy: 1 J), dye laser, wavelength extension units  
Pulse duration: 10 ns  
Wavelength range: 250 nm to 4.5  $\mu$ m
2. High voltage power supplies
3. Residual Gas Analyzer
4. Light Microscopes

## References

- [1] M. Laroussi, and I. Alexeff, " Power Consideration in the Glow Discharge at Atmospheric Pressure", Paper AIAA 99-3667, AIAA Plasmadynamics and Lasers Conf., Norfolk, VA, June 1999.
- [2] Robert H. Stark and Karl H. Schoenbach, "Direct current high-pressure glow discharges," J. Appl. Phys. 85, 2075 (1999).
- \*[3] *Invited Talk*: Rolf Block, Mounir Laroussi, and Karl H. Schoenbach, "Test Facility for High Pressure Plasmas," Proc. IEEE Intern. Conf. Plasma Science, Monterey, CA, June 1999, p. 116.
- \*[4] Rolf Block, Mounir Laroussi, Frank Leipold, and Karl H. Schoenbach, "Optical Diagnostics for Non-Thermal High Pressure Discharges," Proc. 14<sup>th</sup> Intern. Symp. Plasma Chemistry, Prague, Czech Republic, August 1999, Volume II, p. 945.
- \*[5] Karl H. Schoenbach "Electron Density Measurements Using Electrical Probes", Internal Report
- [6] Robert H. Stark and Karl H. Schoenbach, "Direct Current Glow Discharges in Atmospheric Air," Appl. Phys. Lett. 74, 3770 (1999).
- \*[7] Olaf Toedter and Rolf Block, "Gas Temperature Measurement Based on Emission Spectroscopy (Rotational Spectrum of the Second Positive System of Nitrogen)", Internal Report
- \*[8] Rolf Block, Olaf Toedter, and Karl H. Schoenbach, "Gas Temperature Measurements in High Pressure Glow Discharges in Air," Proc. 30<sup>th</sup> AIAA Plasmadynamics and Lasers Conf., Norfolk, VA, July 1999, paper AIAA-99-3434.
- \*[9] Frank Leipold, Robert H. Stark, Ahmed El-Habachi, Karl H. Schoenbach, "Electron Density and Temperature Measurements in an Atmospheric Pressure Air Plasma by Heterodyne Interferometry," Bull. APS, Vol. 44, No. 4, p. 24 (Proc. GEC, Norfolk, VA, October 1999, Paper ETP3 31).
- [10] J.M. Regt, R.D. Tas and J.A.M. van der Mullen, "A diode laser absorption study on a 100 MHz argon ICP," J. Phys. D 29, 2404 (1996).
- \*[11] Olaf Toedter "Gas Temperature Measurement Using Laser Absorption Spectroscopy", Internal Report
- \*[ ]: Enclosed in this Report

# **Test Facility for Atmospheric Pressure Plasmas**

**Grant No: F49620-98-1-0347**

## **Reprints**

## Electron Density Measurements Using Electrical Probes

A relatively simple method to obtain (approximate) values of the electron density in glow discharges is based on current and voltage measurements. Such measurements can be considered standard in electrical discharge experiments [1,2]. The current density in a nonmagnetic plasma, with ion contribution neglected, is  $J = new = en\mu E$ , where  $n$  is the electron density,  $e$  the electron charge,  $w$  the electron drift velocity and  $\mu$  the electron mobility. As discussed in section 1, "Microwave Studies of the Properties of Ionized Gases", the electron energy distribution in ionized gases,  $f$ , can be described by a two term (Legendre) expansion, if elastic collisions dominate. The equation for the current density in ionized gases (equ. 2 in section 1) contains the expression for the electron mobility,  $\mu$ :

$$\mu = -(4\pi/3) (e/m) \int v^3 \partial f_0 / \partial v / (v_m + j\omega) dv \quad (1)$$

The isotropic part of the distribution function,  $f_0$ , is not necessarily Maxwellian (see. Fig. 1 in section 1). It is, particularly for molecular gases, strongly dependent on the reduced field,  $E/N$ . Consequently, the electron mobility is not a constant but also depends on the

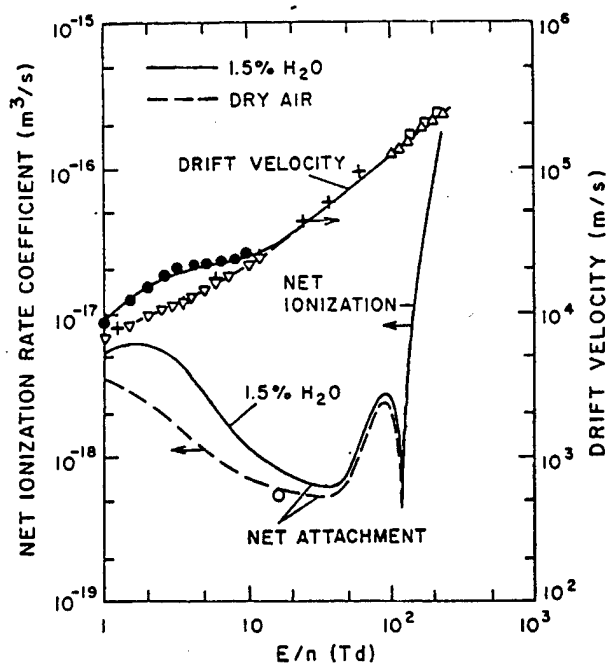


Fig. 1. The lower curves and point show the net attachment and ionization rate coefficients for dry and moist air (1.5%  $H_2O$ ) at a density of  $2.69 \cdot 10^{25} m^{-3}$ . The upper curves and points are the drift velocities of electrons in dry and moist air [3].

reduced field. This is shown in Fig. 1, where the drift velocity (mobility,  $\mu$ , times electric field,  $E$ ), for electrons in atmospheric pressure air at room temperature for dry and moist

(1.5% H<sub>2</sub>O) air dependent on E/N [3] is plotted. The lower limit of E/N in Fig. 1 is 1 Td, which for atmospheric pressure air corresponds to an electric field of 270 V/cm. Drift velocities in air at lower E/N have been measured by Hegerberg and Reid [4] at gas densities between  $1 \cdot 10^{23} \text{ m}^{-3}$  to  $3.3 \cdot 10^{23} \text{ m}^{-3}$  (2.8 Torr to 9.3 Torr at room temperature). The data are shown in figure 2, together with those from other sources [5].

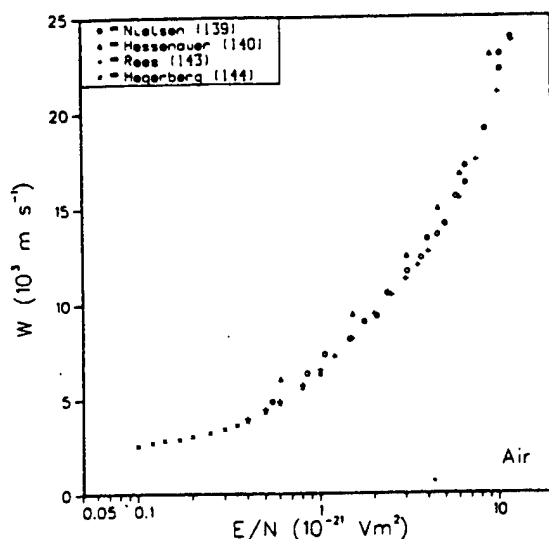


Fig. 2. Drift velocity for electrons in air as a function of E/N [5]

Electric field and current density values can be derived from voltage and current values, and the discharge geometry, assuming homogeneous plasma. The discharge cross-section can be obtained by visual observation. Although the method will only provide values of the electron density, averaged over a large volume, it might in many cases be useful for a quick estimate, before more accurate diagnostic methods are employed.

A similar diagnostic technique, which, however, allows obtaining spatially resolved values of the electron density, was introduced by Johnsen [6]. By using an electrical probe he was able to measure electron densities in the range from  $10^5$  to  $10^{10} \text{ cm}^{-3}$  in photo-ionized gases. The method is based on the measurement of the resistance of the plasma between two electrodes with dimensions small compared to the discharge plasma. The electric probe and its equivalent circuit are shown schematically in Fig. 3 [6].

The electron density is obtained in the same way as described before, through current and voltage measurements. The spatial resolution is determined by the size of the probe. In Johnsen's experiment [4] the cylindrical probe dimensions were on the order of one centimeter.



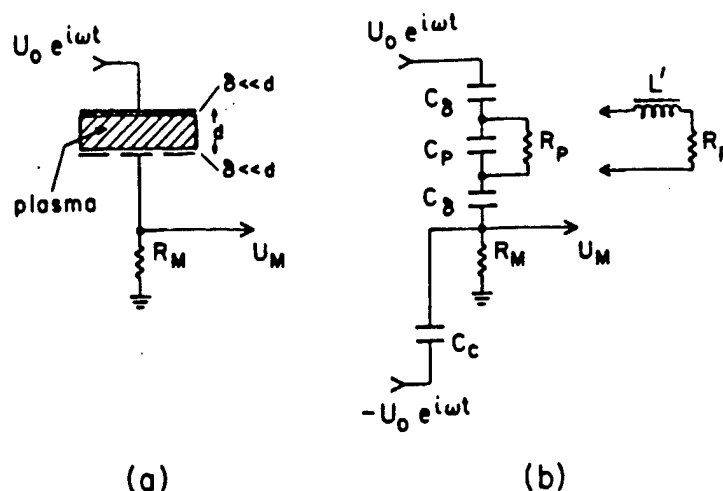


Fig. 3. a) Illustration of the rf probe principle. A weakly ionized plasma fills the space between the plane-parallel conducting electrodes except for the boundary layer with thickness  $\delta$ . A rf voltage is applied to the upper electrode. The current to the lower electrode segment is measured by the voltage drop produced on the resistor  $R_M$ . b) Equivalent electrical circuit, in which  $C_p$  and  $R_p$  symbolize capacitance and resistance of the plasma layer, and  $C_\delta$  stands for the capacitance of the electrodes with respect to the plasma. For a higher approximation, the series combination of  $L'$  and  $R_p$  should be substituted for  $R_p$ .

## Summary

The electrical probe method provides a relatively simple means to obtain information on electron densities in glow discharges through current and voltage measurements. The upper value of the electron density in the experiment described in ref. 6 ( $10^{10} \text{ cm}^{-3}$ ), is not an upper limit of the electron density values obtainable with this diagnostic technique. The method requires knowledge of the electron drift velocity or electron mobility, respectively. Reliable values of the electron drift velocity seem to be for air only available at room temperature. Measurements in air plasmas at higher gas temperature can therefore with the available drift velocity data only provide estimates of the electron density.

Instead of using rf, the measurements can also be performed using short electrical voltage pulses. The pulse width of the applied voltage pulse and the temporal response of the voltage and current probes determine the temporal resolution. The spatial resolution is determined by the size of the double probe. A reduction in size below that of Johnsen's probe is possible. The measurements described in ref. 4 were performed in photo-ionized helium. Measurement in electrical discharges would require a floating probe, and the interpretation of the results would need to take the electric field in the discharge into account.

## References

1. D. Kind, An Introduction in High-Voltage Experimental Technique, Vieweg Verlag, Braunschweig, 1978.
2. Fast Electrical and Optical Measurements, NATO ASI Series, J.E. Thompson and L.H. Luessen, eds, Martinus Nijhoff Publishers, Dordrecht, 1986.
3. A.V. Phelps, "Excitation and Ionization Coefficients," in Gaseous Dielectrics V, L.G. Christophourou and D.W. Bouldin, eds., Pergamon Press, 1
4. R. Hegerberg and I.D. Reid, *Aust. J. Phys.* **33**, 227 (1980).
5. J.W. Gallagher, E.C. Beaty, J. Dutton, and L.C. Pitchford, "An Annotated Compilation and Appraisal of Electron Swarm Data in Electronegative Gases," *J. Phys. Chem. Ref. Data* **12**, 109 (1983).
6. R. Johnsen, "rf-probe method for measurements of electron densities in plasmas at high neutral densities," *Rev. Sci. Instrum.* **57**, 428 (1986).

## Gas Temperature Measurement Based on Emission Spectroscopy (Rotational Spectrum of the Second Positive System of Nitrogen)

### 1. Emission Spectroscopy (Rotational States)

Molecules have quantum states associated to rotation and vibration in addition to the electronic structure. Therefore transitions of the following type will occur:

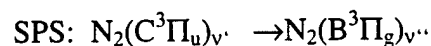
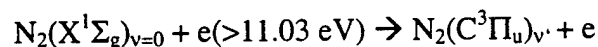
- 1) Rotational, where the vibrational and the electronic state stay constant. Rotational transitions occur in the far infrared and cannot be observed for symmetric molecules like nitrogen.
- 2) Vibrational – Rotational, where the electronic state does not change. The observed spectra are in the infrared region between 20 and 2  $\mu\text{m}$ .
- 3) Electronic transitions, where all states change. The emission is in the visible and near infrared.

Because of the small energies necessary for the rotational stimulation and the short transition times ( $\approx 0.6\text{ns}$ ) molecules in the rotational states and the neutral gas are in equilibrium. Measurements of the rotational temperature consequently provide also the value of the gas temperature [1].

Measurements of the rotational temperature are performed by means of emission spectroscopy. The measured spectrum depends on the thermal population of the rotationally excited states, the matrix elements of the dipole moments between the two states which define the optical transition, and the lineshape function of the spectral system [3]. In order to obtain information on the rotational (gas) temperature the experimental spectrum is compared to a modeled spectrum.

### Modeling of the spectrum for $\text{N}_2$ ( $\text{C} \rightarrow \text{B}$ )

The rotational spectrum has been modeled for nitrogen, which is with 80% the major gas component in air. It contributes to more than 98% of the UV emission in air [3]. The most important transition group in nitrogen is the so-called second positive system, which involves transitions from the electronic C-state to the B-state.



$$\lambda(v'=0 \rightarrow v''=0) = 337.1 \text{ nm}$$

With both vibrational states being zero, the total frequency of a transition is described as the sum of the frequencies of the electronic transition and the difference between two

rotational states [1]. For the three branches P ( $\Delta J = +1$ ), Q ( $\Delta J = 0$ ), and R ( $\Delta J = -1$ ), J being the rotational quantum number, this can be written as:

$$P: \nu_{\Omega,J}^P = \nu_0 + F'_{\Omega,J-1} - F''_{\Omega,J} \quad \text{with } \Omega = 0,1,2$$

$$Q: \nu_{\Omega,J}^Q = \nu_0 + F'_{\Omega,J} - F''_{\Omega,J} \quad \text{with } \Omega = 1,2$$

$$R: \nu_{\Omega,J}^R = \nu_0 + F'_{\Omega,J+1} - F''_{\Omega,J} \quad \text{with } \Omega = 0,1,2$$

with  $F'_{\Omega,J}$  the term values of the rotational states. For the triplet system of nitrogen (total rotational momentum projection  $\Omega=0,1,2$ ) these values can be estimated using the empirical equation of Bud $\wedge$  [1,4]

$$F_{0,J} = B_0 \left( J(J+1) - \sqrt{Z_1} - 2Z_2 \right) - D_v \left( J - \frac{1}{2} \right)^4$$

$$F_{1,J} = B_0 \left( J(J+1) + 4Z_2 \right) - D_v \left( J + \frac{1}{2} \right)^4$$

$$F_{2,J} = B_0 \left( J(J+1) + \sqrt{Z_1} - 2Z_2 \right) - D_v \left( J + \frac{3}{2} \right)^4$$

with  $B_0$  and  $D_v$  the rotational constants obtained from references [4-6]. Equations for the values  $Z_1$  and  $Z_2$  as a function of the spin axis coupling are shown below:

$$Z_1 = Y_v(Y_v - 4) + \frac{3}{4} + 4J(J+1)$$

$$Z_2 = \frac{1}{3Z_1} \left( Y_v(Y_v - 1) - \frac{4}{9} - 2J(J+1) \right)$$

$Y_v$  is the spin-axis coupling constant. Values can be found in references [4-6]. The set of equations allows us to determine the frequencies of the optical transitions.

The population of the rotational states is determined by the Boltzmann distribution :

$$F_J = \frac{N_{v,J}}{N_v} = \frac{(2J+1) \exp\left\{ - (hcB_v J(J+1)/kT) \right\}}{\sum_{J=0}^{\infty} (2J+1) \exp\left\{ - (hcB_v J(J+1)/kT) \right\}}$$

where  $(2J+1)$  is the degeneracy of the quantum state J, and  $B_v$  is a rotational constant depending on the vibrational state. The infinite sum can be approximated by an integral and the population of the rotational states can be described as:

$$N_J = (2J+1) \exp\left( - J(J+1) \frac{B_v hc}{kT} \right)$$

Fig. 1 shows the distribution of rotationally excited states  $N_J$  for three rotational temperatures:

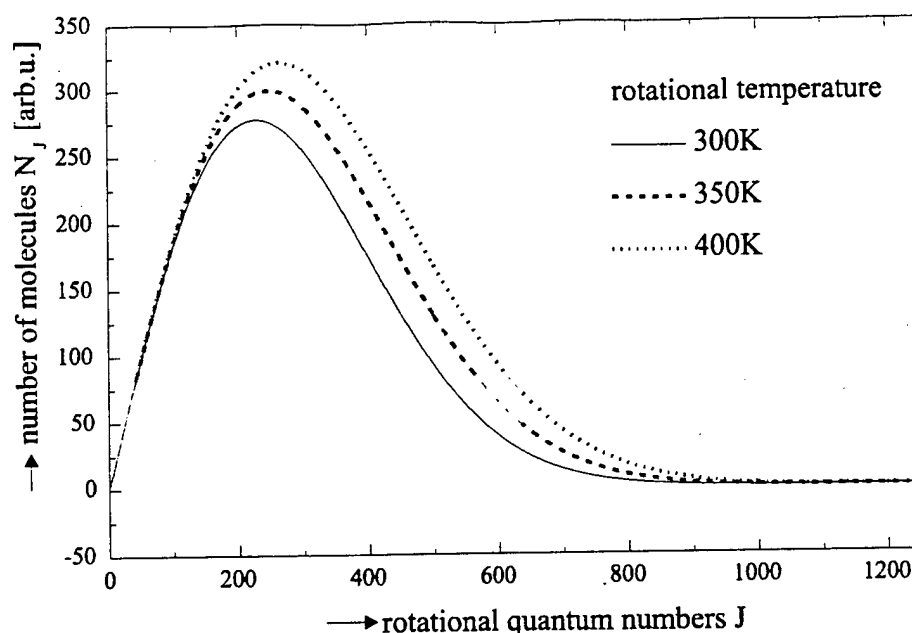


Fig 1: Boltzmann distribution of rotationally excited states

The transition moment can be represented as a product of an electronic only component, a vibrational overlap (Franck-Condon factor) and in a rotational branch strength factor (Hoenl-London factor) [7]. Numerical values for these factors can be found in references [4-6].

The intensity of a spectral line is proportional to the product of the thermal distribution in the upper excited state and the transition moment. In order to obtain the rotational spectrum the instrument broadening needs to be considered. Natural line broadening can generally be neglected. Results of the modeling of the second positive system of nitrogen are shown in Fig. 2.

Generally, the resolution of the rotational structure requires a monochromator with high resolution. However, it is possible even with a system of moderate resolution to obtain information on the temperature. An example is given in the following, where it was assumed, that the resolution of the spectrograph, the instrumental lineshape function was less than required for the resolution of the rotational structure. Figure 3 shows simulation results for such a case, where the lineshape value was 0.15 nm.

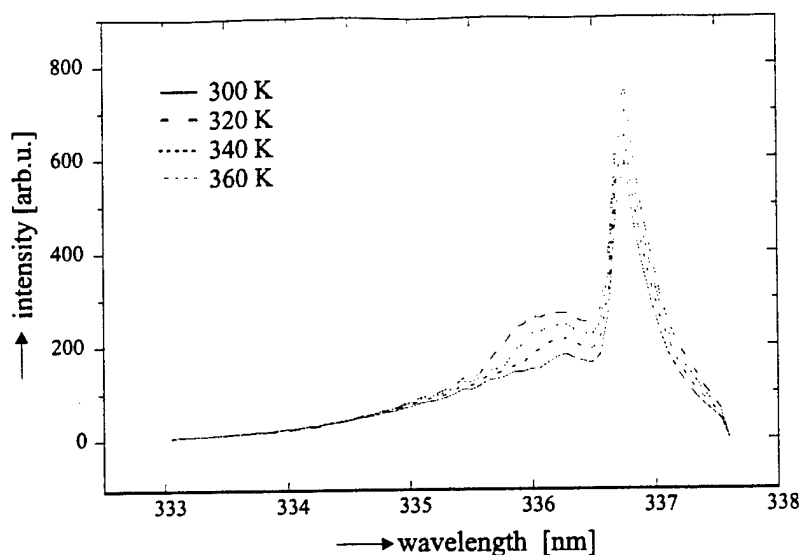


Fig.3: Simulated spectral line of second positive system at several temperatures for an instruments profile 0.15 nm.

By comparing the intensity of the maximum with the local minimum of the rotational spectrum the temperatures at least for low gas temperatures can be obtained (Figure 4).

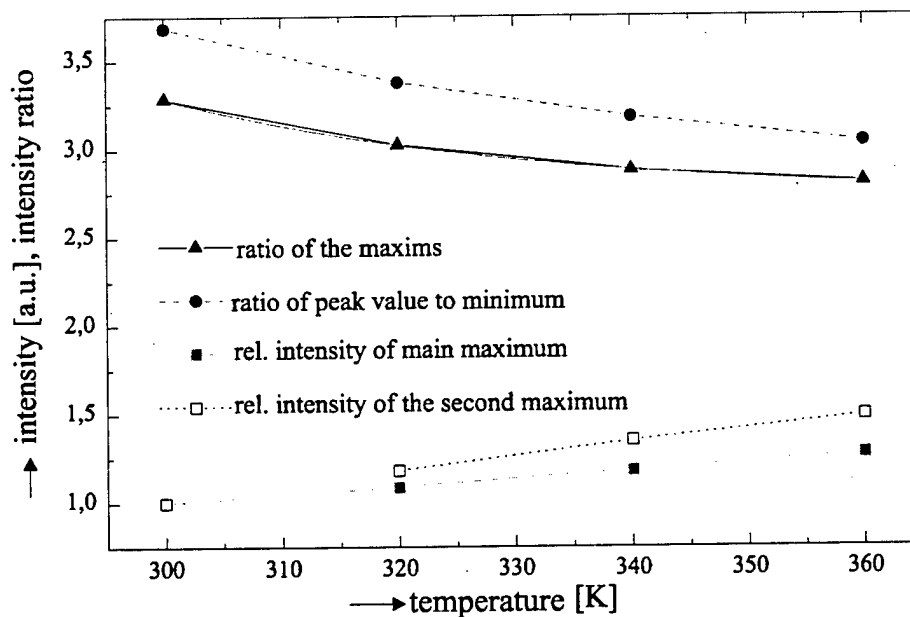
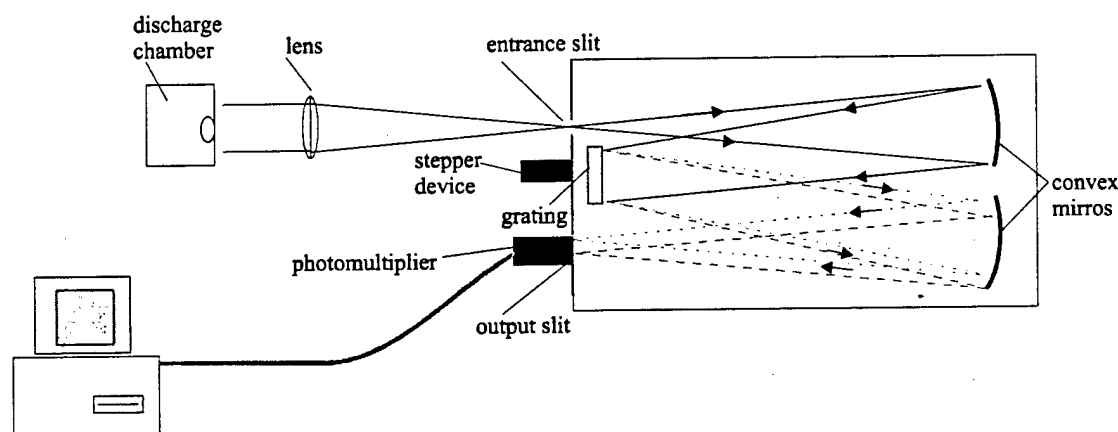


Fig. 4: Dependence of the intensity ratio (main maximum to minimum) on the temperature for an instrument profile of 0.15 nm [10]

It is obvious from these data that this method is limited to values of  $T$  near room temperature. This is the case for pulsed glow discharges. For dc glow discharges we expect much higher temperatures. In order to measure higher temperatures the resolution of the spectral system needs to be increased such that the rotational spectrum can be resolved.

## Experimental Setup (Fig. 5)

Measurements on microhollow cathode discharges in air have been performed in order to demonstrate the diagnostic method. A 0.5m Czerny-Turner spectrograph with a 3600 lines/millimeter grating is used as dispersing element. The collimating mirror is 3" in diameter and the focussing mirror is 6" in diameter. With the grating dimensions of 50\*50 mm a linear dispersion of 4.15 / mm is achieved. Using a 10  $\mu\text{m}$  entrance slit the maximum achievable resolution is 0.1. A photomultiplier is used as detector. The electrical signal of the photomultiplier is recorded by an AD converter card and displayed on a monitor. Figure 5 shows the schematics of the experimental setup.



*Fig. 5: Experimental setup*

Figure 8 shows an example of the rotational structure of the second positive system of nitrogen for dc microhollow cathode discharges at three discharge currents [11]. The temperatures for these discharges are estimated. The development of a correlation technique which will allow us to determine the temperatures more accurately is underway.

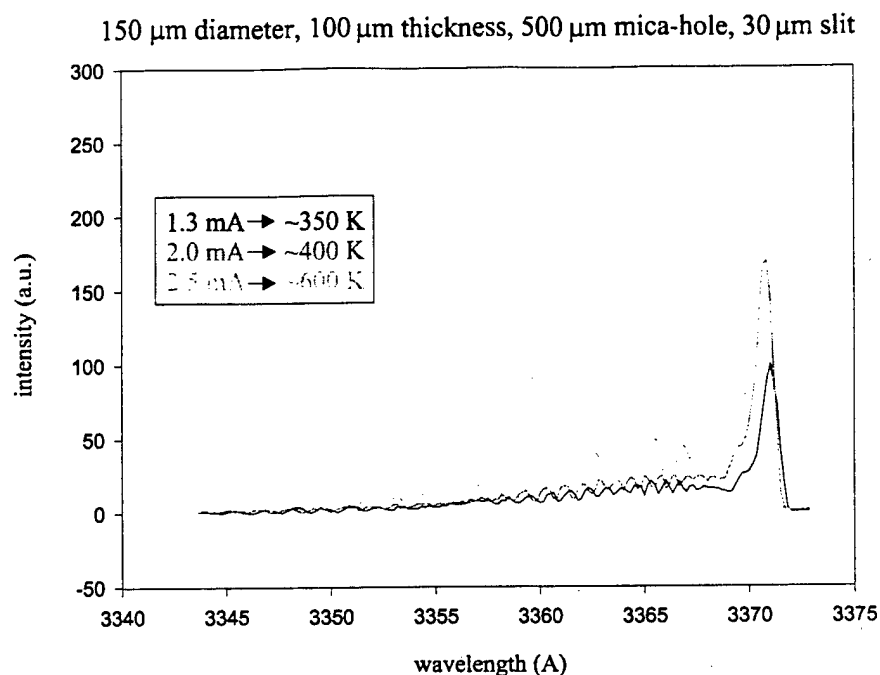


Fig. 8: Experimentally obtained rotational spectrum of microhollow cathode discharge in air at 170 Torr. The instrument profile was 0.02 nm.

## References

- [1] Herzberg, G. "Molecular Spectra and Molecular Structure, Volume I: Spectra of Diatomic Molecules," Krieger, 1950
- [2] A. Unsöld, "Physik der Sternatmosphären," Springer, 1955
- [3] C.L.M. Creighton, "Pulsed Positive Corona Discharges," Ph.D thesis, TU Eindhoven, 1995
- [4] A. Budde "Die Rotationskonstanten B, D und Y der  $^3\Pi$ -Terme von  $\text{TiO}$ ,  $\text{C}_2$ ,  $\text{CO}$ ,  $\text{PH}$ ,  $\text{AlH}$ ,  $\text{NH}$ ," Z. Physik, **97**, 437 (1936).
- [5] A. Lofthus and P.H. Krupenie, "The spectrum of molecular nitrogen," J. Phys. Chem. Ref. Data, **6**, 113 (1977).
- [6] G. Bittenger and G. Herzberg, "Über die Struktur der zweiten positiven Stickstoffgruppe und die Prädissoziation des  $\text{N}_2$ -Moleküls," Annalen d. Physik, **21**, 577 (1935).
- [7] D.L. Huestis, Radiative Transition Probabilities, in Atomic, Molecular and Optical Physics Handbook, G.W.F. Drake, ed. American Institute of Physics, 1996.



- [8] D.M. Phillips, Determination of gas temperature from unresolved bands in the spectrum from a nitrogen discharge, J. Phys. D, 1975, **8**, p.507
- [9] A. Czernichowsky, "Temperature evaluation from the partially resolved 391 N<sub>2</sub>-Band," J. Phys. D, **20**, 559 (1987).
- [10] O. Toedter, "Untersuchungen zur Korona-Entladung als Beschichtungsverfahren," Ph.D. thesis, Universität des Saarlandes, Saarbrücken, 1998.
- [11] O. Toedter, R. Block and K.H. Schoenbach, "Temperature Measurements on Microhollow Cathode Discharges in Air," to be published.

## Gas Temperature Measurements Using Laser Absorption Spectroscopy (O. Toedter)

The shape of spectral lines is determined by line broadening processes. The most important processes in atmospheric pressure gases are Doppler and pressure broadening, already described in section 3 of the "Electron Density Measurement" manuscript. Doppler broadening is related to the kinetic energy of gas atoms and molecules. Measurements of the Doppler profile of an spectral line allows us therefore to obtain information on the gas temperature.

The spectral line profile is a convolution of Lorentz and Gauss functions. The resulting profile, a Voigt profile, includes the pressure broadening in its Lorentz part and Doppler broadening in its Gauss part. By using a numerical deconvolution method [5] for the Voigt profile the gas temperature can be determined directly from the full width at half maximum of the Gaussian shape, the Doppler width of the line,  $\Delta\lambda_D = 2\pi c/\omega_D$ , where  $\omega_D$  is given as:

$$\omega_D = \omega_0 \sqrt{\frac{2kT}{Mc^2}}$$

In order to resolve the line profile, absorption spectroscopy can be used. Since absorption measurements are line-of-sight measurements information on the local values of the gas temperature requires observation of the discharge at various angles. Only in the case of cylindrical symmetry a simple evaluation of the local temperature values is possible by means of Abel inversion.

The source that is used for absorption measurements needs to have a line width small compared to the width of the examined line. If a spectral lamp is used as light source a monochromator is required to provide the necessary spectral resolution. A simpler and generally more precise method is to use a tunable monochromatic light source such as a diode laser. Diode lasers emit a spectral line with a width in the range of several picometers. They are available in a wide range of wavelengths and power levels.

A common method used to modulate the center wavelength of the laser diode is through variation of temperature. However, mode hopping limits the application of this method in temperature controlled diodes (Fig. 1). Therefore, generally the selection of the laser mode is done by adjusting the temperature, and the fine-tuning of the wavelength by modulation of the diode current (Fig. 2) [4].

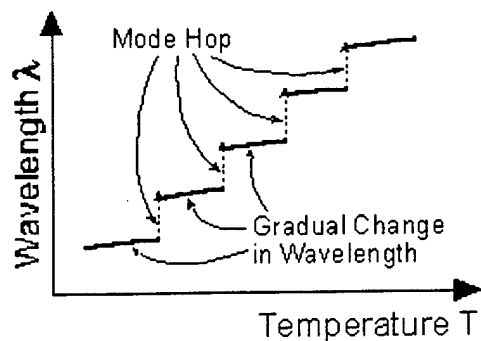


Fig 1 Center wavelength change with temperature

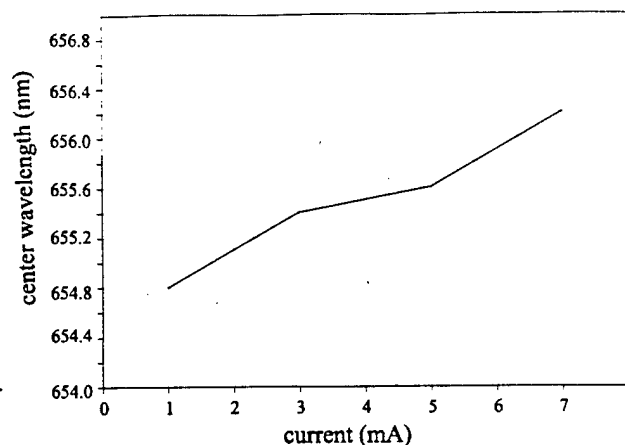


Fig. 2 Center wavelength change with current

Index guided laser diodes are best suited for these measurements. The spectral line has a narrow Lorentzian shape and the wavelength is only slightly dependent on the injected current, which allows precise fine-tuning. The laser diode should be temperature controlled at about 1mK [6]. There are two methods which can be used to obtain a high temperature resolution:

- Using large heat sinks and regulation circuits of high accuracy but large time constants.
- Using small heat sinks with small thermal capacity and fast bidirectional control electronics, e.g. a pulse width modulated Peltier element.

In both cases an accurate measurement of the temperature is important. Semiconductor temperature sensors have shown good results.

In order to get a non-convoluted absorption profile, the laser must be index guided with a bandwidth of  $\Delta\lambda$  less than 0.1 pm. The current controller and the connection must be designed for a stability better than 1 mA. The spectral line width can be reduced by means of an external resonator [1] such as a Littrow grating reflecting in the first order. Mounted at a lever for a sensitive handling the grating only reflects the first order of the spectral centerline into the internal cavity of the semiconductor laser. Tilting the lever results in a change of the cavity length:

$$\Delta d_c = L \cos \alpha \cdot \Delta \alpha ,$$

causing a wavelength change of :

$$\Delta \lambda = (\Delta d_c / d_c) \cdot \lambda$$

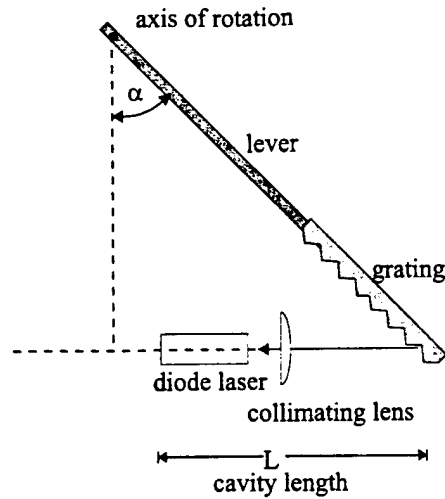


Fig 4: Schematics of an external cavity diode laser arrangement

The wavelength of the laser diode needs to be calibrated with respect to its current and its stability needs to be checked. The wavelength calibration can be performed by means of a low pressure argon discharge lamp in connection with a Fabry-Pérot interferometer. The data acquisition could be performed by means of an AD-converter, which feeds into a computer.

An example of this diagnostic technique applied to an argon plasma is given in the following [6]. For measurements of the gas temperature in an air plasma the same procedure could be used. By adding a small amount of argon to air the  $4s-4p$  transition of argon at 811.531 nm ( $4s^3P_2 - 4p^3D_3$ ) could be utilized. Fig. 3 shows the calculated Doppler width as a function of the gas temperature for this particular transition.

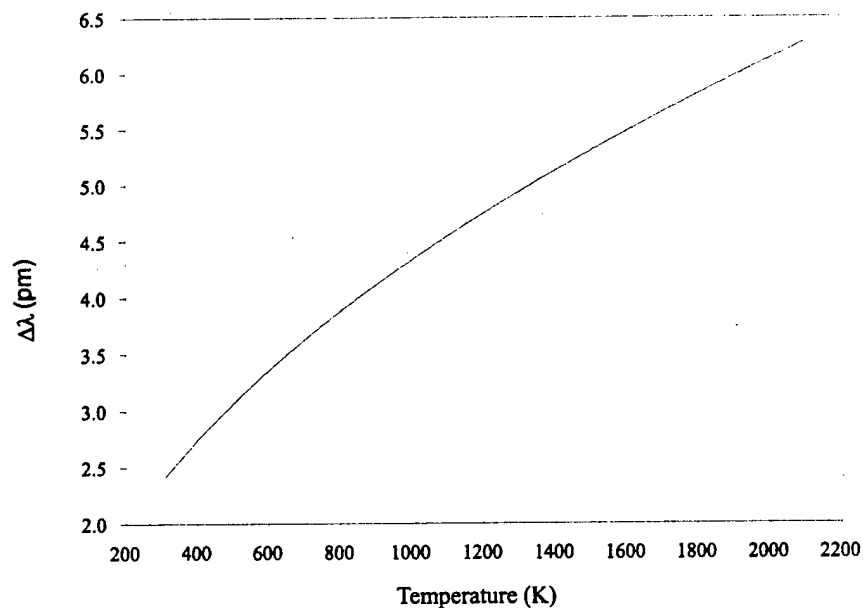


Fig 3: Calculated doppler broadening as function of temperature (argon 4s-4p)

The experimental set-up would be similar to that used by de Regt et al [6] to measure the gas temperature in a high pressure argon plasma (Fig. 4). The diode laser had a maximum output power of 30 mW at a maximum operation current of 85.8 mA. The bandwidth was < 0.1 pm.

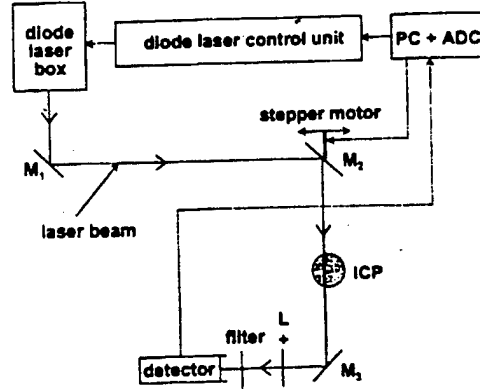


Fig. 4 The experimental set-up of the diode laser absorption diagnostics. The diode laser beam is led by mirrors, M1, M2 and M3 through the plasma and to the detector. Lens L focuses the beam for all lateral positions onto the detector. A PC with ADC controls both the laser wavelength and the position of mirror M2 to select the lateral position [6].

The laser intensity,  $I_\lambda$ , after passing through a plasma of thickness,  $d$ , in de Regt's case an inductively coupled plasma (ICP), is given as:

$$I_\lambda(d) = I_0 \exp[-\tau(\lambda)] + S_\lambda \{1 - \exp[-\tau(\lambda)]\}$$

Where  $I_0$  is the initial laser intensity,  $\tau(\lambda)$  is the optical depth, and  $S_\lambda$  is the source function of the measured transition.  $S_\lambda$  can be obtained by measuring the intensity of the plasma without a laser beam. The optical depth, which can be obtained by comparing  $I_\lambda(d)$  with  $I_0$ , is given as the integral of the absorption coefficient,  $\kappa(\lambda)$ , over the line of sight:

$$\tau(\lambda) = \int \kappa(\lambda) dx$$

An absorption profile obtained this way is shown in Fig. 5 [6].

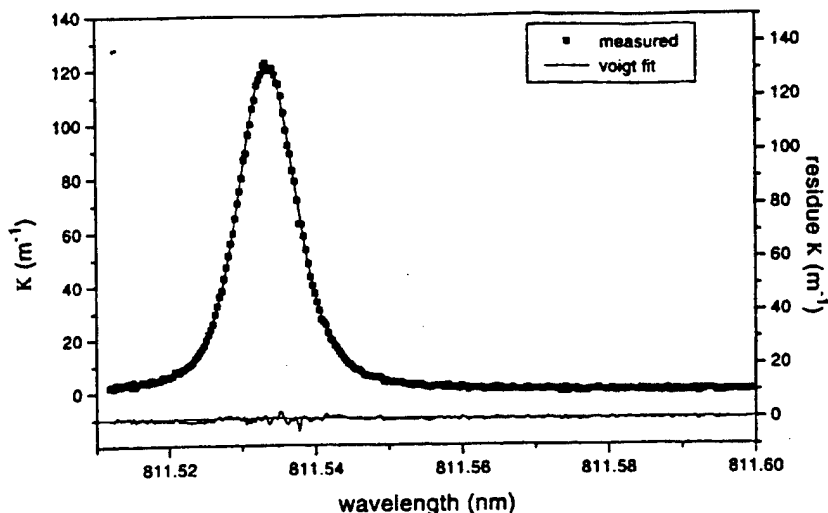


Fig. 5. An example of an absorption profile with the absorption coefficient  $\kappa(\lambda)$  as a function of the wavelength at one radial position at 7 mm ALC (after Abel inversion) and the corresponding Voigt fit [6].

After the line profile is obtained (e.g. after an Abel inversion, if the plasma is cylindrical) a least-mean-squares fitting program is used to adjust the measurements to a Voigt profile. The results of the fit give the width of the Gaussian and Lorentzian parts of the profile. The width of the Gaussian profile is then used to calculate the temperature of (in the discussed example) the argon atoms in the 4s state, which is identical to the temperature of the atoms in the ground state. Fig. 7 shows the results of such calculations [6]. The resolution in this experiment was about 500 K.

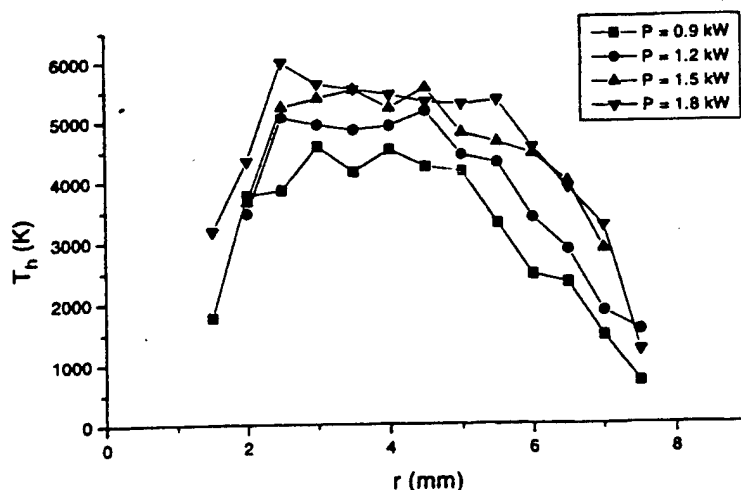


Fig. 7. Heavy particle temperatures for different input powers as a function of the radius at 7 mm ALC. In the high temperature region of the profiles the inaccuracies are about 10 % [6].

## References

- [1] W. Demtröder, Laser Spectroscopy, Springer, 1995.
- [2] H.R. Griem, "Spectral Line Broadening by Plasmas" in Pure and Applied Physics Vol. 39, Academic Press, 1974.
- [3] H.R. Griem, Principles of Plasma Spectroscopy, Cambridge University Press, 1997.
- [4] H. Kressel and J.K. Butler, Semiconductor Lasers and Heterojunction LED's, Academic Press, 1977.
- [5] P. A. Jansson, Deconvolution of Images and Spectra, Academic Press, 1997.
- [6] J.M. Regt, R.D. Tas and J.A.M. van der Mullen, "A diode laser absorption study on a 100 MHz argon ICP," *J. Phys. D* **29**, 2404 (1996).

## 2B01-2

Invited -

### Test Facility for High Pressure Plasmas

Rolf Block, Mounir Laroussi & Karl H. Schoenbach, Old Dominion University, Norfolk, VA 23529, USA

### Test Facility for High Pressure Plasmas\*

Rolf Block, Mounir Laroussi, and Karl H. Schoenbach  
Physical Electronics Research Institute/ Appl. Research Center  
Old Dominion University, Norfolk/ Newport News, VA

High pressure nonthermal plasmas are gaining increasing importance because of their wide range of applications, e.g. in air plasma ramparts, gas processing, surface treatment, thin film deposition, and chemical and biological decontamination. In order to compare various methods of plasma generation with respect to efficiency, development of instabilities, homogeneity, lifetime etc., a central test facility for high pressure plasmas is being established.

The facility will allow us to study large volume ( $> 100 \text{ cm}^3$ ), nonthermal (gas temperature:  $< 2000 \text{ K}$ ) plasmas over a large pressure range ( $10^{-6}$  Torr up to more than 1 atmosphere) in a standardized discharge cell. The setup was designed to generate plasmas in air as well as in gas mixtures. The available voltage range extends to 25 kV dc (10 kW power). The electrodes can be water cooled.

Electrical diagnostics include a 400 MHz, 2 GS/s 4-channel oscilloscope for current and voltage measurements and the detection of the onset of instabilities.

For optical diagnostics, a CCD video camera is used to record the appearance of dc discharges. A high-speed light intensified CCD-camera (25 mm MCP with photocathode, gating speed: 200 ps, adjustable in 10 ps steps) allows to study the development of instabilities and can also be utilized in temporally resolved spectroscopic measurements.

Optical emission spectroscopy allows us to determine plasma parameters such as electron density (through Stark broadening measurements) and gas temperature measurements. We have particularly concentrated our efforts on gas temperature diagnostics. The rotational structure of the second positive system of nitrogen contains information on the neutral gas temperature, which is identical with the rotational temperature [1]. Taking the apparatus profile into account, the temperature of the rotational excited molecules is determined by a comparison of simulated and measured data. A spectrograph with an instrument profile of  $\text{FWHM}=0.1 \text{ \AA}$  is available.

Interferometry is well suited for electron density measurements especially in weakly ionized plasmas. A 4 mm microwave interferometer will be used for this diagnostics. Number densities up to  $7 \cdot 10^{13} \text{ cm}^{-3}$  can be measured in this wavelength range. For higher densities we plan to use an IR interferometer with a  $\text{CO}_2$  laser as source.

\* Funded by the Air Force Office of Scientific Research in Cooperation with the DDR&E Air Plasma MURI Program.

[1] Rolf Block, Olaf Toedter and Karl H. Schoenbach, "Temperature Measurement in Microhollow Cathode Discharges in Atmospheric Air", Bull. APS 43, No. 6, NW1 2, p. 1478, 1998.



# OPTICAL DIAGNOSTICS FOR NON-THERMAL HIGH PRESSURE DISCHARGES

Rolf Block, Mounir Laroussi, Frank Leipold, and Karl H. Schoenbach  
Physical Electronics Research Institute/Applied Research Center  
Old Dominion University  
12050 Jefferson Ave.  
Newport News, VA 23606

## Abstract

Two important parameters of high pressure, non-thermal plasmas are the gas temperature and the electron density. Optical emission spectroscopy and laser interferometry have been used to obtain these parameters in a dc atmospheric pressure hollow cathode discharge in air. Temperatures at and below 2000K and electron densities of approximately  $10^{16} \text{ cm}^{-3}$  have been measured. The two diagnostic methods are a subset of techniques developed to characterize non-thermal, high pressure plasmas in a newly established test facility at Old Dominion University.

## 1. Introduction

Non-thermal, high pressure plasmas have recently been used in novel emerging applications such as excimer light sources [1], surface modification of polymers [2], biological decontamination [3], and air plasma ramparts [4,5]. Each of these applications requires a specific set of plasma parameters. Diagnostic techniques applicable for high-pressure plasmas are required to adequately characterize the discharge. In this paper, we concentrate on a spectroscopic method, which yields information on the rotational structure of the second positive system of nitrogen for gas temperature measurement, and on interferometric methods using IR or microwave sources for electron density measurement. The experimental setups are presented, and results obtained on plasma generated with a microhollow cathode discharge are discussed.

## 2. Temperature Measurement

Optical emission spectroscopy allows us to determine plasma parameters such as electron density (through Stark broadening measurements) and gas temperature measurements. We have particularly concentrated on the gas temperature diagnostics in non-equilibrium plasmas in air. The rotational structure of the second positive system of nitrogen (transitions from the electronic

C-state to the B-state) contains information on the rotational temperature. Because of the low energies needed for rotational excitation and the short transition times, molecules in the rotational states and the neutral gas molecules are in equilibrium. Consequently, the rotational temperature provides also the value of the neutral gas temperature.

The 0-0 band of the second positive system of molecular nitrogen, modeled as a rigid rotor, has been simulated with the rotational temperature as variable parameter. In order to determine the plasma temperature, the simulated spectra are compared with the measured one. This comparison requires that the instrument profile (FWHM) of the spectrograph has to be taken into account. This is done by convoluting the computed line spectra with the appropriate Gauss function. Such simulated spectra for an FWHM=0.02nm are shown in fig. 1 for three temperatures [6]. The curves are shifted vertically for a better separation.

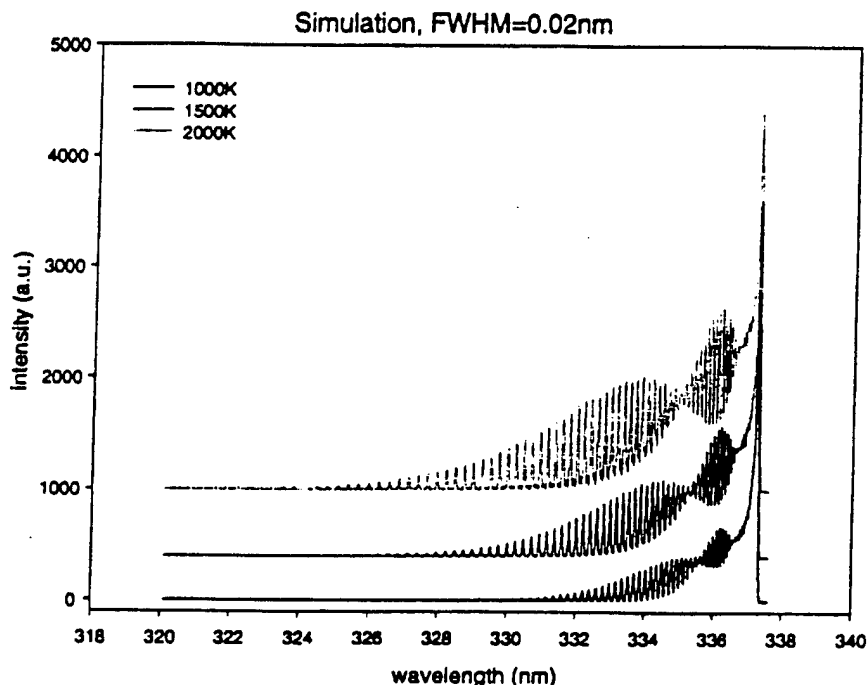


Fig. 1: Simulated spectra of molecular nitrogen

Generally, resolving the rotational structure requires a monochromator with very high resolution. A 0.5m imaging monochromator/spectrograph with a 3600 g/mm grating (with 240nm blaze wavelength) was used as dispersing element. Dual exit ports offer the versatility of mounting two different detectors at the same time. One exit port is equipped with an exit slit and a photomultiplier. The second port will be used for a fast light-intensified CCD-camera (25mm micro channel plate with photocathode, gating speed down to 200ps, adjustable in 100ps steps), which allows temporally resolved spectroscopic measurements.

Fig. 2 shows a measured spectrum of a microhollow cathode discharge (MHCD) in room air at atmospheric pressure. A MHCD is a direct current, high pressure glow discharge between two closely spaced electrodes, which contain circular openings [7]. The electrodes are separated by an insulator (mica or alumina). In this experiment we used 100 $\mu$ m thick molybdenum

electrodes, separated by a 125 $\mu\text{m}$  thick sheet of alumina, with 100 $\mu\text{m}$  holes. The dc voltage across the electrodes was 380V, the discharge current was 12mA. The instrument profile of the spectrograph was measured with a mercury lamp (line at 361nm) as FWHM=0.02nm. A comparison with simulated spectra resulted in a temperature of  $T=1500\text{K}$ .

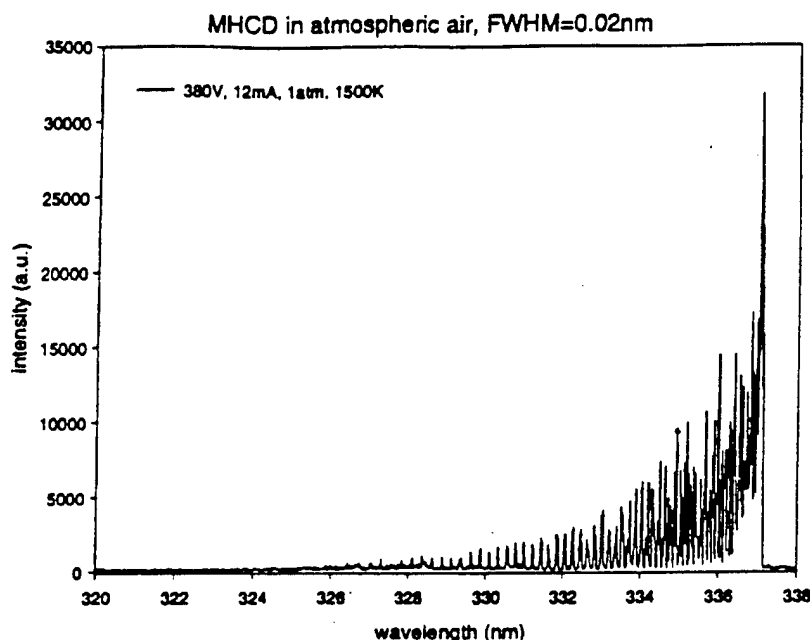


Fig. 2: Measured spectrum of a MHCD in atmospheric air.

The nitrogen line at 337.1nm (within the second positive system of nitrogen) is the line with the highest intensity and therefore easy to measure. This diagnostic can also be used in other gas mixtures, if the application allows the addition of small amounts of nitrogen.

### 3. Electron Density Measurement

#### 3a. Infrared Interferometry

The interferometer is designed as a heterodyne Mach-Zehnder interferometer. The source is a  $\text{CO}_2$ -laser operating at 10.6 $\mu\text{m}$ . Figure 3 shows the experimental setup.

The laser beam is split in two beams. One beam passes through the plasma, while the second beam passes along a reference path, where it undergoes a frequency shift of 40 MHz applied by an acousto-optic modulator. Using a beam splitter, the two beams are allowed to interfere and produce two signals, only one of which has the beat frequency of 40 MHz. This signal is then compared to the driver signal of the acousto-optic modulator (which also has a frequency of 40 MHz). The phase shift is then converted to a voltage by a phase detector. The resolution of the interferometer was about 0.01 degree.

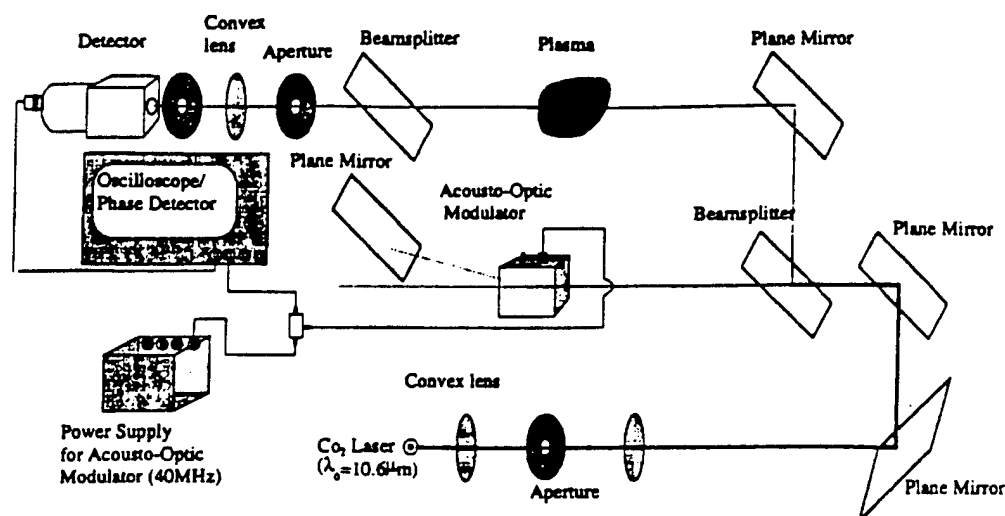


Fig. 3: IR-Interferometer for electron density measurement

The above-described technique is best applied to a pulsed system, with pulse repetition rate of few kilohertz. This enables the separation of the phase shift caused by the electrons from the phase shift caused by mechanical movement and thermal drifts. This method was applied to plasma generated by a microhollow cathode discharge in atmospheric pressure room air, using a sample with the same dimensions (100 $\mu\text{m}$  thick molybdenum electrodes, separated by 125 $\mu\text{m}$  thick alumina sheet, with 100 $\mu\text{m}$  holes). The voltage between the electrodes was 390V, the discharge current was 12mA. The plasma was 100 $\mu\text{m}$  wide and 400 $\mu\text{m}$  long. Electron densities on the order of  $10^{16} \text{ cm}^{-3}$  were measured. In order to provide evidence that the laser does not affect the plasma in the micro cavity, experiments with varying laser intensity have been performed. Fig. 4 shows that the electron density measurements are independent of the laser beam power.

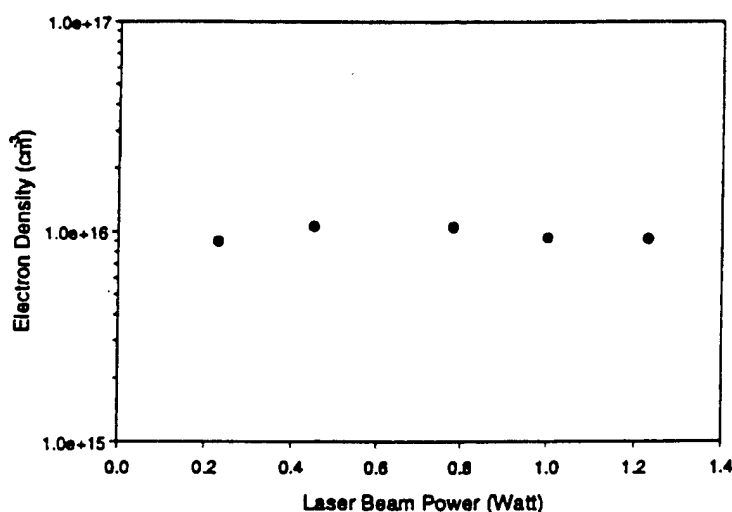


Fig. 4: Electron density versus laser beam power

### 3b. Microwave Interferometry

In order to extend the range of electron density measurements to lower values, a microwave interferometer is being developed. The increase in wavelength allows us to expand the diagnostic range down to  $10^{12} \text{ cm}^{-3}$ , however on the expense of spatial resolution. Figure 5 shows the interferometer design we adopted for our experiments.

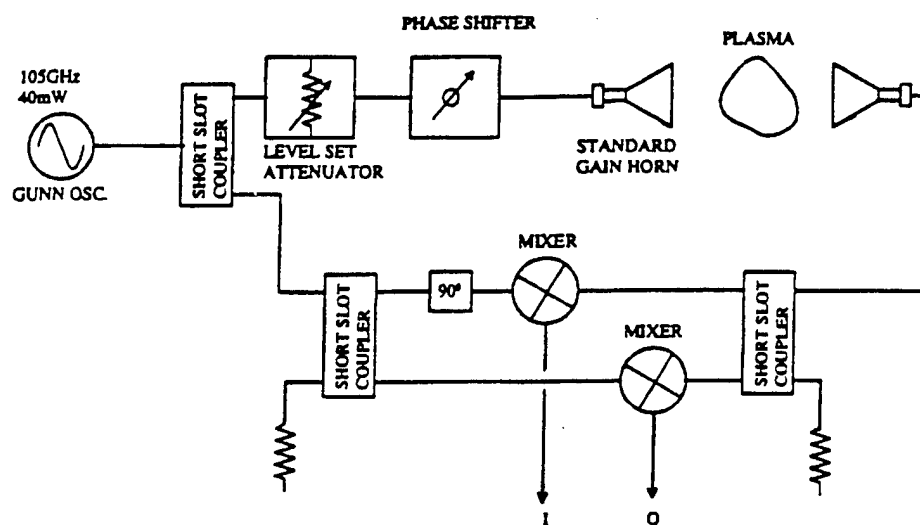


Fig. 5: Microwave Interferometer for number density measurement

The microwave interferometer, or phase bridge, shown above operates as follows. A microwave signal generated by a Gunn diode oscillator is divided in two equal portions by a Short Slot Coupler. One portion is transmitted through the plasma. The second portion is channeled to a second power divider which splits the signal to drive the LO input of the I-Q mixers. The signal transmitted by the plasma is also split in two portions, which drive the RF inputs of the I-Q mixers. Since both the LO and RF inputs of the mixers are at the same frequency, a DC signal is obtained at the IF output of the mixers. Calibration of the bridge is achieved by setting the Level Set Attenuator to the maximum attenuation position, measuring the DC offset of the mixers, varying the Phase Shifter through  $360^\circ$ , and recording the DC voltage at the IF output of the mixers. The measurement is repeated for varying level of attenuation. This set of data is then used to analyze actual phase shifts undergone by the microwave signal with the plasma ON. The accuracy of the measurement is determined by the resolution of the voltage measurements.

### Conclusion

Spectroscopic measurements of the structure of the second positive system of nitrogen allow us to accurately determine the background gas temperature in nonthermal plasmas. Our method was used on a microhollow cathode discharge. Temperatures at and below 2000 K were measured. Infrared and microwave interferometry allow us to obtain information on the electron

number density over a wide range. Using the IR interferometer on a microhollow cathode discharge plasma, we measured electron densities close to  $10^{16} \text{ cm}^{-3}$ . A specially designed microwave interferometer will allow us to measure electron densities down to about  $10^{12} \text{ cm}^{-3}$ .

The diagnostic techniques presented in this paper are a part of a test facility for high pressure, non-thermal plasmas. This test facility allows to study large volume plasmas over a large pressure range in a standardized discharge cell. The facility also includes electrical (large bandwidth scopes for current-voltage measurements) and optical (high speed CCD camera to study the development of instabilities) diagnostics.

### Acknowledgement

This work was funded by the US Air Force Office of Scientific Research in Cooperation with the DDR&E Air Plasma MURI Program.

### References

- [1] Ahmed El-Habachi and Karl H. Schoenbach, "Generation of Intense Excimer Radiation from High-Pressure Hollow Cathode Discharges", *Appl. Phys. Lett.* **73**, (1998), 885.
- [2] F. Massines, C. Mayoux, R. Messaoudi, A. Rabehi, and P. Segur, "Experimental Study of an Atmospheric Pressure Glow Discharge: Application to Polymers Surface Treatment", *Proc. Int. Conf. Gas Discharges & their Applications*, 1992, 730.
- [3] M. Laroussi, "Sterilization of Contaminated Matter with an Atmospheric Pressure Plasma", *IEEE Trans. Plasma Sci.*, **24**, (1996), 1188.
- [4] M. Laroussi, "Interaction of Microwaves with Atmospheric Pressure Plasmas", *Int. J. IR & Millimeter Waves*, **16**, (1995), 2069.
- [5] Robert H. Stark and Karl H. Schoenbach, "A Novel Plasma Cathode for High Pressure Glow Discharges", *J. Appl. Phys.*, **85**, (1999), 2075.
- [6] Rolf Block, Olaf Toedter and Karl H. Schoenbach, "Temperature Measurement in Microhollow Cathode Discharges in Atmospheric Air", *Bull. APS*, **43**, October 1998, 1478.
- [7] Karl H. Schoenbach, Ahmed el-Habachi, Wenhui Shi and Marco Ciocca, "High Pressure Hollow Cathode Discharges", *Plasma Sources, Science and Technology*, **6**, (1997), 468.



**AIAA 99-3434**

**Gas Temperature Measurements in High Pressure  
Glow Discharges in Air**

Rolf Block, Olaf Toedter and Karl H. Schoenbach

Old Dominion University

Norfolk, VA

**30th Plasmadynamics and Lasers Conference**  
**28 June - 1 July, 1999 / Norfolk, VA**

## GAS TEMPERATURE MEASUREMENTS IN HIGH PRESSURE GLOW DISCHARGES IN AIR

Rolf Block, Olaf Toedter, and Karl H. Schoenbach\*  
Physical Electronics Research Institute/Applied Research Center  
Old Dominion University, Norfolk, VA, 23529/Newport News, VA 23606

### ABSTRACT

The temperature of the neutral particles in weakly ionized air can be determined by measuring the rotational spectrum of the 0-0 band within the second positive system of nitrogen and comparing it with simulated spectra. This diagnostic technique has been applied to direct current microhollow cathode discharges in atmospheric air. Temperatures in the range from 1700K to 2000K have been measured over a discharge current range from 4mA to 12mA. The rotational spectra of nitrogen were simulated using a simple model, which can easily be implemented. The simplicity compensates for the loss in accuracy (~10%), which can be achieved with more sophisticated models.

### INTRODUCTION

High-pressure glow discharges are nonequilibrium discharges: The temperature of the heavy particles is generally much less than the electron temperature. Applications for high pressure glow discharges range from gas lasers, remediation and detoxification of gaseous pollution, biological decontamination, surface treatment and thin film deposition, to their use as plasma ramparts. These are atmospheric pressure air plasmas, which serve as shields against strong electromagnetic radiation, and can be activated on a time scale of less than microseconds.

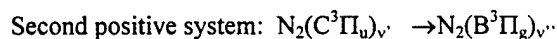
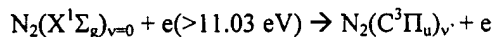
Of the plasma parameters which need to be known in order to determine the use of the air plasmas as ramparts two are of utmost importance: the electron density and the gas temperature. The electron density determines the frequency range where the shield is effective; the gas temperature should be below 2000K in order to prevent thermal loading of the system which is to be protected. A method, which allows us to obtain the temperature of the heavy particles in air, is based on

the measurement of the rotational state distribution in the second positive system of nitrogen, which involves transitions from the electronic C-state to the B-state. Due to the low rotational excitation energies and the short transition times (~0.6ns) the temperature relaxation between rotationally excited molecules and the neutral gas is very fast. Consequently, the rotational temperature provides a value for the neutral gas temperature, too.

Measurements of the rotational temperature are performed by means of emission spectroscopy. The measured spectrum depends on the thermal distribution of the rotationally excited states, the probability for the optical transitions, and the line shape function of the spectral system. In order to obtain information on the rotational (gas) temperature, the measured spectrum is compared to a simulated spectrum.

### SIMULATION OF THE N<sub>2</sub> SPECTRUM

The 0-0 band of the second positive system of molecular nitrogen has been simulated with the rotational temperature as variable parameter. Nitrogen, which is with 80% the major gas component in air, contributes to more than 98% of the UV emission in low temperature glow discharges. The strongest transition group in nitrogen is the so-called second positive system, which involves transitions from the electronic C-state to the B-state.



$$\lambda(v'=0 \rightarrow v''=0) = 337.1 \text{ nm}$$

The diatomic molecule of nitrogen is modeled as a symmetric top (rigid rotator). With the quantum number of both vibrational states being zero, the total frequency of a transition is described as the sum of the frequencies of the electronic transition and the difference between two rotational states. For the three branches P ( $\Delta J = +1$ ),

- 
- Professor, Department of Electrical and Computer Engineering
  - Copyright © 1999 The American Institute of Aeronautics and Astronautics Inc. All rights reserved.



Q ( $\Delta J=0$ ), and R ( $\Delta J=-1$ ), J being the rotational quantum number, this can be written as<sup>1</sup>:

$$P: \nu_{\Omega,J}^P = \nu_0 + F_{\Omega,J'-1} - F_{\Omega,J''} \quad \text{with } \Omega = 0,1,2$$

$$Q: \nu_{\Omega,J}^Q = \nu_0 + F_{\Omega,J'} - F_{\Omega,J''} \quad \text{with } \Omega = 1,2$$

$$R: \nu_{\Omega,J}^R = \nu_0 + F_{\Omega,J'+1} - F_{\Omega,J''} \quad \text{with } \Omega = 0,1,2$$

where  $\nu_0$  is called the band origin or the zero line and  $F_{\Omega,J'}$  the term values of the rotational states. For the triplet system of nitrogen (total rotational momentum projection  $\Omega=0,1,2$ ) these values can be estimated using the semiempirical equation of Budó<sup>2</sup>:

$$F_{0,J'} = B_v \left( J'(J'+1) - \sqrt{Z_1} - 2Z_2 \right) - D_v \left( J' - \frac{1}{2} \right)^4$$

$$F_{1,J'} = B_v \left( J'(J'+1) + 4Z_2 \right) - D_v \left( J' + \frac{1}{2} \right)^4$$

$$F_{2,J'} = B_v \left( J'(J'+1) + \sqrt{Z_1} - 2Z_2 \right) - D_v \left( J' + \frac{3}{2} \right)^4$$

with  $B_v$  and  $D_v$  being the rotational constants obtained from reference<sup>3,4</sup>. Equations for the values  $Z_1$  and  $Z_2$  as a function of the spin-orbit coupling constant  $Y_v$  are shown below:

$$Z_1 = Y_v(Y_v - 4) + \frac{3}{4} + 4J'(J'+1)$$

$$Z_2 = \frac{1}{3Z_1} \left( Y_v(Y_v - 1) - \frac{4}{9} - 2J'(J'+1) \right)$$

$Y_v$  takes the transition for increasing  $J'$  from Hund's case (a) to Hund's case (b) into account. Values can be found in references<sup>5,6</sup>. This set of equations allows us to determine the frequencies of the optical transitions.

The temperature dependent population of the rotational states for  $J'$  as well as  $J''$  is determined by the Boltzmann distribution:

$$f_J = \frac{N_{v,J}}{N_v} = \frac{(2J+1) \exp\left\{-\left(\frac{hcB_v J(J+1)}{kT}\right)\right\}}{\sum_{J=0}^{\infty} (2J+1) \exp\left\{-\left(\frac{hcB_v J(J+1)}{kT}\right)\right\}}$$

where  $(2J+1)$  is the degeneracy of the quantum state J and  $B_v$  is a rotational constant depending on the vibrational state. The infinite sum can be approximated by an integral, and the population of the rotational states can be described as:

$$f_J = \frac{hcB_v}{kT} (2J+1) \exp\left(-J(J+1) \frac{B_v hc}{kT}\right).$$

The intensity of each upper rotational level can be expressed, apart from a constant, as the product of the Boltzmann distribution  $f_J$  and a line-strength factor  $S_J$ , which defines the distribution over the P, Q and R branches. The precise formulae for the line strengths of

a symmetric top for absorption, which are valid whether or not thermal equilibrium exists, were first given by Hönl and London<sup>7</sup>:

$$S_{J',P} = \frac{(J'+1+\Omega)(J'+1-\Omega)}{J'+1}$$

$$S_{J',Q} = \frac{(2J'+1)\Omega^2}{J'(J'+1)}$$

$$S_{J',R} = \frac{(J'+\Omega)(J'-\Omega)}{J'}$$

The relative intensity of a spectral line is the product of the thermal distribution in the upper excited state and the Hönl-London factors:

$$I_{rel} = S_{J'} \cdot f_J$$

These formulas allow us to calculate the relative rotational line spectrum (wavelengths and intensities) of molecular nitrogen. In order to compare the measured spectrum with computed spectra, line-broadening effects have to be taken into account. Natural line broadening can be neglected compared to the instrumental FWHM. The instrument profile is measured using a low-pressure mercury lamp. In the last simulation step the computed line spectrum is convoluted with a Gaussian distribution with the FWHM determined in the calibration measurement. Results of the simulation of the line at 337.1 nm within the second positive system of nitrogen for an instrumental FWHM=0.025 nm at several temperatures are shown in fig. 1. The curves are shifted vertically for a better separation.

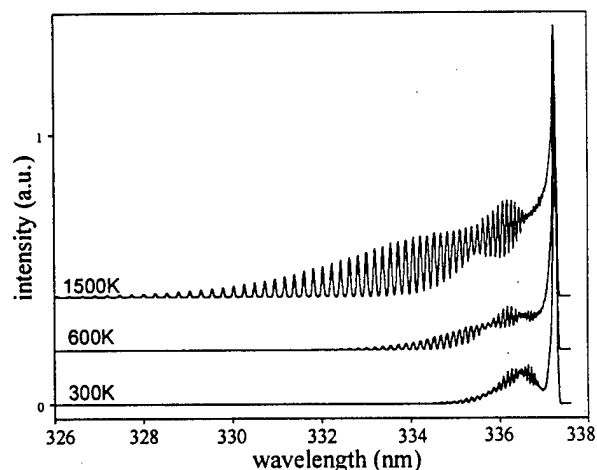


Fig. 1: Simulated (0-0) band of the second positive system of nitrogen at 300K, 600K and 1500K.

The diagnostic method has been applied to microhollow cathode discharges<sup>8</sup> in atmospheric air.

## EXPERIMENTAL RESULTS

Microhollow cathode discharges (MHCDs) are direct current, high pressure glow discharges between two closely spaced electrodes, which contain circular openings. In this experiment two 100  $\mu\text{m}$  thick circular molybdenum electrodes were used, which were separated by a 130  $\mu\text{m}$  thick alumina layer. A laser drilled hole through the sample had a cathode hole diameter of 170  $\mu\text{m}$ . The anode hole diameter is smaller. Experiments have shown that the anode geometry does not affect the discharge considerably; the anode hole could even be omitted. In order to keep the capacitance of the electrodes small, the cathode had a much smaller diameter than the anode. Details of the sample are shown in fig. 2.

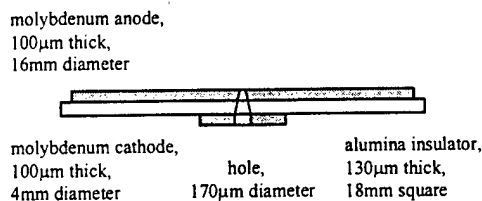


Fig. 2: Microhollow cathode geometry

The electrical circuit and the experimental setup are shown in fig. 3.

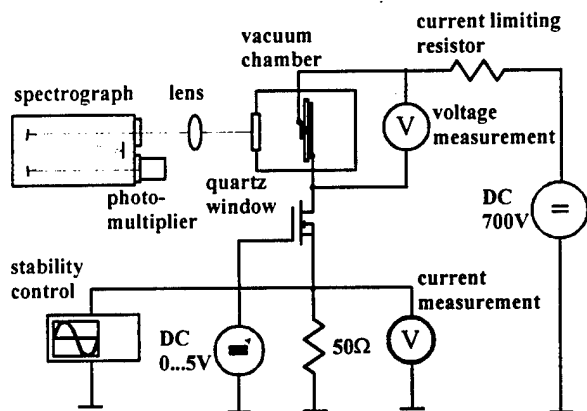


Fig. 3: Experimental setup

The Mosfet acts as a constant current source. The constant drain current can be adjusted by changing the dc gate voltage. The discharge is ignited by

momentarily raising the drain supply voltage. The sample is mounted in a stainless steel vacuum chamber.

A 0.5m Czerny-Turner spectrograph with a 3600 grooves/mm grating blazed at 240nm is used to record the emission spectrum. A photomultiplier with a spectral range of 180nm – 900nm is attached to the output slit. The electrical signal of the photomultiplier is recorded via a 16bit AD converter card. The instrumental FWHM was determined using the lines at 365nm and 312nm of a low-pressure mercury lamp; a resolution of 0.24 $\text{\AA}$  was achieved. A measured spectrum from 300nm to 450nm of the discharge in atmospheric pressure dry air is shown in fig. 4. It shows the second positive system of nitrogen with the strongest line at 337.1nm.

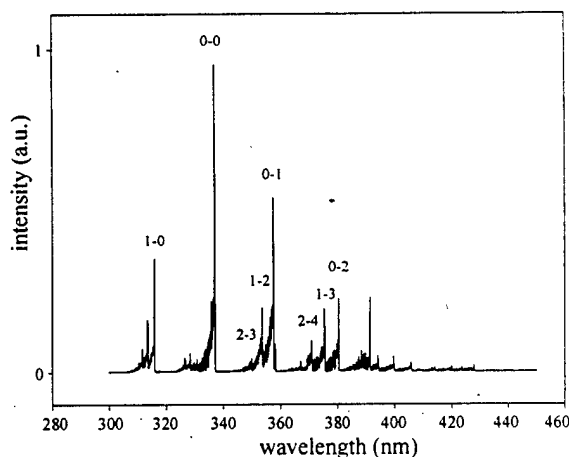


Fig. 4: Emission spectrum of MHCD in atmospheric air

Rotational spectra of microhollow cathode discharges at atmospheric pressure in dry air as well as normal room air have been measured for various discharge currents. In order to prove that a thermal steady state is reached, measurements were repeated over time. Starting 10 minutes after igniting the discharge and adjusting the current to 4mA, 3 consecutive measurements in intervals of 10 minutes have been performed. Then the current was adjusted to 8mA and finally to 12mA, with the same measurement procedure for each current. Results for dry air are shown in fig. 5. The spectra are normalized and vertically shifted for a better separation.

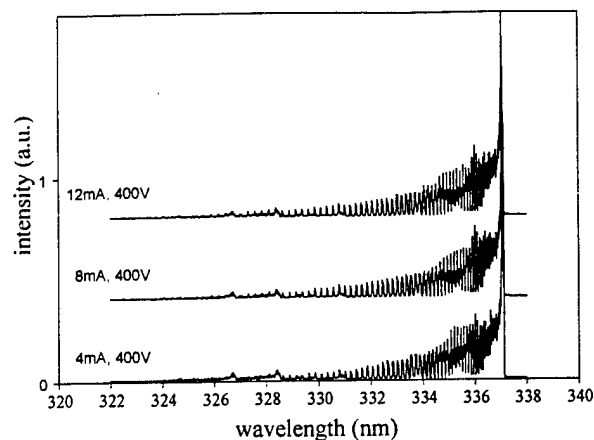


Fig. 5: Measured rotational spectra of MHCDs in dry air at atmospheric pressure.

With increasing temperature, higher rotational states are excited. In order to determine the highest temperature in the plasma, only the higher rotational states for wavelengths below 330nm were compared with the computed spectra. With increasing discharge currents from 4mA to 8mA and to 12mA the highest gas temperature increases from 1700K to 1900K and to 2000K. Although the power is doubled from 4mA to 8mA (the voltage is constant) and increased again by a factor of 1.5 from 8mA to 12mA, the temperature changes only by about 15%. This is probably due to the fact that with increasing power the plasma volume increases, so that the power density is only slightly changed.

The same measurements have been performed for room air (humid air). The results show the same behavior, with slightly smaller temperature changes (highest and average temperature) over the discharge current.

## CONCLUSION

The neutral gas temperature in weakly ionized air can be estimated by a comparison of measured and simulated spectra of the (0-0) band of molecular nitrogen. The  $N_2$  molecule was modeled as a rigid rotator, which allows a very easy implementation. However, the simplified model causes a loss in accuracy especially at higher temperatures. One measurement on a microhollow cathode discharge at a high temperature has shown that for temperatures up to 2000K the accuracy is about 10%. Our estimated

temperature was found to be lower by this fraction, compared to the results of a more sophisticated model<sup>9</sup>. This derivation from actual values is expected to be less for lower temperatures.

## ACKNOWLEDGEMENTS

This work was supported by the U.S. Air Force Office of Scientific Research in cooperation with the DDR&E Air Plasma Ramparts MURI program, and by the Department of Energy, Advanced Energy Division.

## REFERENCES

- <sup>1</sup> Herzberg, G., "Molecular Spectra and Molecular Structure, Volume I: Spectra of Diatomic Molecules", D. van Nostrand Company, Inc, Princeton, New Jersey, 1950.
- <sup>2</sup> Budó, A., "On the triplet-band term formulas for the general intermediate case and their application to the  $B^3\Pi$  and  $C^3\Pi$  terms of the  $N_2$  molecule", Z. Physik. 96, 1935, p. 219.
- <sup>3</sup> Roux, F., Michaud, F., and Vervloet, M., "High-resolution Fourier spectrometry of  $14N_2$ : Analysis of the (0-0), (0-1), (0-2), (0-3) bands of the  $C^3\Pi_u-B^3\Pi_g$  system", Can. J. Phys. 67, 1998, p. 143.
- <sup>4</sup> Roux, F., Michaud, F., and Verloet, M., "High-resolution Fourier spectrometry of  $14N_2$  violet emission spectrum: Extension of the analysis of the  $C^3\Pi_u-B^3\Pi_g$  system", J. Mol. Spec. 158, 1993, p. 270.
- <sup>5</sup> Lofthus, A., and Krupenie, P.H., "The spectrum of molecular nitrogen". J. Phys. Chem. Ref. Data, 6, 1977.
- <sup>6</sup> Herzberg, G., and Buettendbender, G., "Ueber die Struktur der zweiten positive Stickstoffgruppe und die Praedissoziation des  $N_2$ -Molekuelns", Annalen der Physik, 21, 1935, p. 577.
- <sup>7</sup> Hönl, H., and London, F., Z. Physik 33, 1925, p. 803.
- <sup>8</sup> Schoenbach, K. H., El-Habachi, A., Shi, W., and Ciocca, M., "High Pressure Hollow Cathode Discharges", Plasma Sources Science and Technology, 6, 1997, p. 468.
- <sup>9</sup> Laux, Christophe, Stanford University, Thermo-sciences Division, Stanford, CA: private communication.

ETP3 31 Electron Density and Temperature Measurements in an Atmospheric Pressure Air Plasma by Heterodyne Interferometry FRANK LEIPOLD, ROBERT H. STARK, AHMED EL-HABACHI, KARL H. SCHOENBACH, *Old Dominion University, Norfolk, VA 23529* Measurements of the electron density and gas temperature in a microhollow cathode supported (MCS) glow discharge in 1 atmosphere air have been performed by means of a heterodyne CO<sub>2</sub>-laser Mach-Zehnder interferometer. The index of refraction contains contributions from both electrons and heavy particles, and therefore information on the electron density and the density of the neutral and ionized atoms and molecules, respectively. In order to separate the information on electron density and gas temperature we have measured the temporal development of the index of refraction during the ignition phase of the discharge. Since the generation of electrons occurs on a much faster time scale than heating of the gas, the initial fast decay of the index of refraction was assumed to be due to changes in electron density, the following slower decay to be due to increase in temperature. In first experiments on MCS atmospheric pressure air discharges electron densities of  $10^{13}$  to  $10^{14}$  cm<sup>-3</sup> have been measured. The gas temperature at steady-state was found to be between 1500 K and 2500 K. — This work was funded by the Air Force Office of Scientific Research in Cooperation with the DDR&E Air Plasma Ramparts MURI Program and the National Science Foundation.